High-Resolution Probabilistic Projections of Temperature Changes over Ontario, Canada

XIUQUAN WANG

Institute for Energy, Environment and Sustainable Communities, University of Regina, Regina, Saskatchewan, Canada

GUOHE HUANG

Institute for Energy, Environment and Sustainable Communities, University of Regina, Regina, Saskatchewan, Canada, and SC Institute for Energy, Environment and Sustainability Research, North China Electric Power University, Beijing, China

QIANGUO LIN

Key Laboratory of Regional Energy and Environmental Systems Optimization, Ministry of Education, North China Electric Power University, Beijing, China

JINLIANG LIU

Department of Earth and Space Science and Engineering, York University, Toronto, Ontario, Canada

(Manuscript received 25 November 2013, in final form 1 April 2014)

ABSTRACT

Planning of mitigation and adaptation strategies to a changing climate can benefit from a good understanding of climate change impacts on human life and local society, which leads to an increasing requirement for reliable projections of future climate change at regional scales. This paper presents an ensemble of high-resolution regional climate simulations for the province of Ontario, Canada, developed with the Providing Regional Climates for Impacts Studies (PRECIS) modeling system. A Bayesian statistical model is proposed through an advance to the method proposed by Tebaldi et al. for generating probabilistic projections of temperature changes at gridpoint scale by treating the unknown quantities of interest as random variables to quantify their uncertainties in a statistical way. Observations for present climate and simulations from the ensemble are fed into the statistical model to derive posterior distributions of all the uncertain quantities through a Markov chain Monte Carlo (MCMC) sampling algorithm. Detailed analyses at 12 selected weather stations are conducted to investigate the practical significance of the proposed statistical model. Following that, maps of projected temperature changes at different probability levels are presented to help understand the spatial patterns across the entire province. The analysis shows that there is likely to be a significant warming trend throughout the twenty-first century. It also suggests that people in Ontario are very likely to suffer a change greater than 2°C to mean temperature in the forthcoming decades and very unlikely to suffer a change greater than 10°C to the end of this century.

1. Introduction

Climate change is becoming one of the most pressing issues around the world. It has already started to affect every continent, country, community, and individual. As the largest economy in Canada, the province of Ontario is now facing extraordinary challenges under a changing climate. In recent years, people are seeing more frequent and intense weather anomalies, shorter duration of ice cover on lakes, and fluctuating water levels in lakes, rivers, and streams (Ontario Ministry of the Environment 2011a). For example, local residents in southern Ontario suffered the hottest summer yet in 2010, which was deemed the hottest year on record by Environment Canada, leading to an increasing requirement for investments in energy systems, especially in the electricity system (Ontario Ministry of Energy 2010).

Corresponding author address: Guohe Huang, Institute for Energy, Environment and Sustainable Communities, University of Regina, 3737 Wascana Parkway, Regina SK S4S 0A2, Canada.
E-mail: huang@iseis.org.

DOI: 10.1175/JCLI-D-13-00717.1

In response to these challenges, the province of Ontario has been taking prudent steps to protect its health, economy, and communities from the harmful effects of climate change (Ontario Ministry of the Environment 2011b). The realization of such an adaptation initiative substantially depends upon how well we know and how confident we are about the negative impacts of a changing climate in the context of Ontario. It thus leads to the development of reliable climate projections at finer resolutions over the domain of Ontario, aiming at providing decision makers or policy makers with helpful information for assessing plausible future effects of climate change at regional scales.

Forecasts of future climate change with current state-of-the-art climate models can provide potential evidence for decision makers and policy makers to help determine how to adapt to or mitigate climate change. However, these forecasts are inevitably uncertain due to our incomplete understanding of the climate system in terms of its complicated physical processes and natural variability, as well as the response to rising levels of greenhouse gases (Allen et al. 2000; Murphy et al. 2004; Stainforth et al. 2005; Stott and Kettleborough 2002; Webster et al. 2003). This further results in considerable uncertainties about the rates of change that can be expected, such as changes in extremes of temperature and precipitation and sea level rise (Karl and Trenberth 2003). No single model can be powerful enough to tackle such uncertainties all at once, so it is necessary to utilize results from a range of coupled models (Houghton et al. 2001).

Previously, a number of climate research projects based on multimodel ensemble (MME) or perturbed physics ensemble (PPE) approaches have been carried out to explore techniques for quantifying uncertainties of future climate change (e.g., Barnett et al. 2006; Furrer et al. 2007; Giorgi and Francisco 2000; Giorgi and Mearns 2002, 2003; Greene et al. 2006; Harris et al. 2013; Murphy et al. 2007; Sexton et al. 2012; Tebaldi and Sansó 2009; Tebaldi et al. 2005; Watterson and Whetton 2011). The MME approach usually consists of various GCMs developed at different modeling centers around the world to sample both structural and parametric uncertainties to a limited degree (Meehl et al. 2007; Taylor et al. 2012), but it is unable to sample the consequences of either type of uncertainty in a systematic fashion since it is assembled on an opportunistic basis from current available models (Murphy et al. 2007; Sexton et al. 2012). The PPE usually consists of variants of a single base model with perturbed parameters limited in a space of possible model configurations (Collins et al. 2006; Murphy et al. 2004; Webb et al. 2006; Yokohata et al. 2010). The main advantage of the PPE approach is that it allows greater control over the design of experiments to sample parametric uncertainties within a single model framework. Both ensemble approaches can generate a large number of projections of future climate for various scenarios, but how to combine these multiple projections and interpret them into policy-relevant information has become a major challenge in recent years, due to the lack of verification of climate projections, the problems of model dependence, bias, and tuning, and the difficulty in making sense of an ''ensemble of opportunity'' (Knutti et al. 2010; Tebaldi and Knutti 2007).

There are obviously different ways to synthesize modeling results of MMEs or PPEs. A straightforward way is to calculate the multimodel averages for given diagnostics or variables where each model is weighted equally (Räisänen and Palmer 2001). In many cases, combining ensemble results through Bayesian methods or weighted averages, where weights are determined by comparing model predictions to observations, shows improved performance better than simple averages (e.g., Barnston et al. 2003; Krishnamurti et al. 1999, 2000; Robertson et al. 2004). The article by Tebaldi and Knutti (2007) presents a comprehensive literature review on the existing published methods to obtain best estimates of climate change based on multiple projections through ensemble approaches. It concludes that the combined estimates, which are generally expressed in a probabilistic way based on a variety of statistical methods (e.g., Giorgi and Mearns 2002, 2003; Tebaldi et al. 2005), may give more helpful information for impact studies and decision making given that none of the model projections for future climate can be validated at this stage. For example, as each estimate comes with a specific level of occurrence (i.e., probability), it thus allows for planning appropriate adaptation strategies in advance by balancing the tradeoff between the adapting costs and the potential damages of climate change at different probabilistic levels.

However, previous probabilistic studies have mainly focused on quantifying climate change uncertainties at global scales based on various GCM ensembles (e.g., Furrer et al. 2007; Greene et al. 2006; Tebaldi and Knutti 2007; Tebaldi and Sansó 2009). Additional downscaling work needs to be done before feeding the probabilistic projections into impact models (e.g., hydrological modes or crop models) because of the coarse resolution of GCM outputs, by either statistical approaches (e.g., Wang et al. 2013; Wilby et al. 2004) or regional climate models (RCMs) . A small number of papers published in recent years (e.g., Benestad 2004; Luo et al. 2005; Manning et al. 2009; New et al. 2007) have approached the problem of deriving regional probabilistic projections

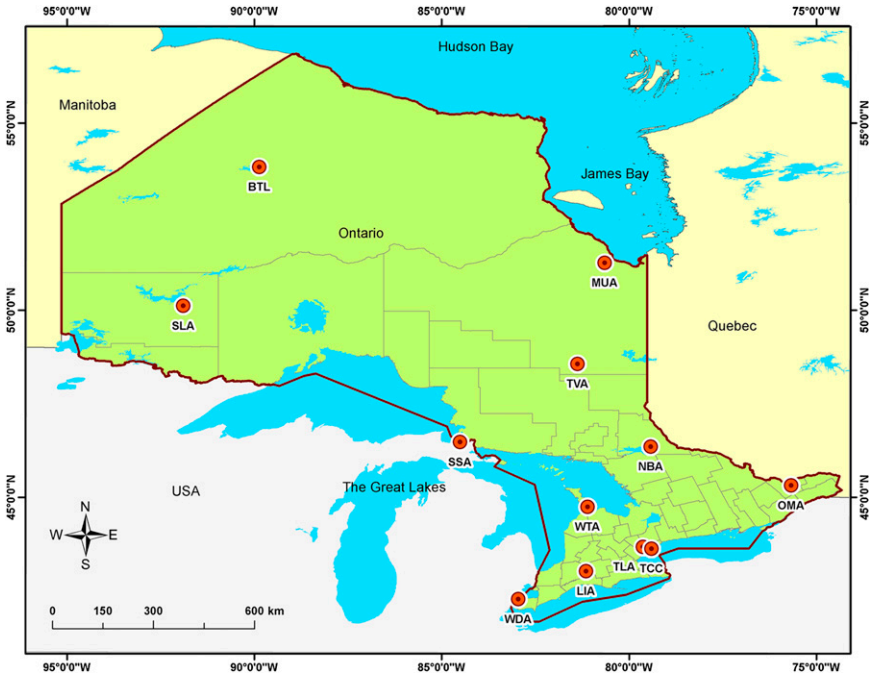

FIG. 1. Map of study area.

at a finer resolution to facilitate the assessment of regional and local climate change impacts, but they are characterized by a less general approach and are tailored to specific regions or impacts studies.

The objective of this research is to develop high-resolution probabilistic projections of temperature changes for the province of Ontario, Canada, where uncertainties in observational errors, model reliability, and temporal correlation of climate change signals will be reflected through a Bayesian hierarchical model. Specifically, a 25-km RCM ensemble is first developed and assembled by using a subset of 17-member PPE ensemble (McSweeney et al. 2012), which is developed based on the Hadley Centre Coupled Model, version 3 (HadCM3), as boundary conditions to drive the Providing Regional Climates for Impacts Studies (PRECIS) regional modeling system (Jones et al. 2004) from 1950 to 2099. A Bayesian statistical model is then advanced based on the method proposed by Tebaldi et al. (2005) for generating probabilistic projections of climate change at grid point scale, by treating the unknown quantities of interest as random variables to quantify their uncertainties in a statistical way. Observations for current climate and simulations of the PRECIS ensemble are fed into the Bayesian model to derive posterior distributions of all the uncertain quantities, which are next used to construct probabilistic projections of temperature changes over Ontario. This paper is organized as follows: section 2 describes the development of RCM ensemble using PRECIS; section 3 details the formulation of a Bayesian hierarchical model; section 4 presents the results including the main findings at 12 selected weather stations and maps of projected temperature changes at different probabilistic levels over the entire province; and the last section summarizes the study and states the main conclusions.

2. Development of RCM ensemble

a. Study area

As the second largest province in Canada, Ontario is located in the east-central area of Canada and covers more than 10^6 km^2. As shown in Fig. 1, Ontario is bounded by Quebec to the east, Manitoba to the west, Hudson Bay and James Bay to the north, and the Great Lakes to the south. With a population of more than 13.5 million, Ontario is home to about 2 in 5 Canadians. More than 85% of the total population lives in urban centers, largely in cities on the shores of the Great Lakes. In summer, temperatures in Ontario can soar above 30°C, whereas in winter they can drop below −40°C. It has been reported by Ontario Ministry of the Environment (2011a) that the average temperature in Ontario has gone up by as much as 1.4°C since 1948. In southern Ontario, the number of days over

30°C will likely more than double by 2050. This will lead to hotter summers with more heat waves. The greatest change will likely take place in the far north in winter. Warmer winters will make it more difficult for wildlife and people in the far north to adapt. For example, some dramatic changes have already started near the coast of Hudson Bay and James Bay. Furthermore, warmer temperatures are causing the loss of permafrost, which may result in changes in the local landscape and the stability of houses and buried water pipes. The water levels in the Great Lakes have been found to be dropping with warmer winters, less ice cover, and hotter summers. This change will directly influence more than 70% of people in the province who depend on the Great Lakes for their drinking water.

In 2007, Ontario introduced its climate change action plan as a framework for action to reduce greenhouse gas (GHG) emissions (Ontario Ministry of the Environment 2011c). Following that, the government of Ontario (Ontario Ministry of the Environment 2011b) reported its adaptation strategy and action plan to create a vision and framework for collaboration across government, businesses, communities, institutes, and individuals, aiming at minimizing the negative impacts of a changing climate by taking prudent actions to adapt well to climate change. Such initiatives require a better understanding of how the climate of Ontario will change in both short and long terms, through a regional climate modeling approach.

b. Regional climate modeling using PRECIS

Regional climate modeling is an essential way for conducting thorough assessments of climate change impacts by providing impact researchers with regional detail of how future climate might change. An RCM is a powerful tool to add small-scale detailed information of future climate change to the large-scale projections of a GCM. RCMs are physics-based climate models and as such represent most or all of the processes, interactions, and feedbacks between the climate system components that are represented in GCMs (Jones et al. 2004). By taking coarse-resolution information from GCMs, RCMs can develop temporally and spatially finescale information using their higher-resolution representation of the climate system. In this study, we apply a widely used RCM developed at the Hadley Centre, PRECIS, to facilitate regional climate modeling over Ontario. PRECIS is a flexible, easy to use, and computationally inexpensive RCM designed to provide detailed climate scenarios (Wilson et al. 2011). It can be applied easily to any area of the globe to generate detailed climate change projections, with the provision of a simple user interface as well as a visualization and data-processing package. PRECIS is able to run at two different horizontal resolutions: 0.44° × 0.44° (approximately 50 km × 50 km) and 0.22° × 0.22° (approximately 25 km × 25 km), with a vertical resolution of 19 atmospheric levels using a hybrid coordinate system (a linear combination of a terrain-following σ coordinate and an atmospheric pressure–based coordinate).

Using a single GCM projection to drive RCMs can provide us with some information about the expected changes under a given emission scenario for the region of interest, but it does not provide us with more information about how confident we should be in those changes (Bellprat et al. 2012). The ensemble approach through either MMEs or PPEs is widely accepted as an effective way to explore the range or spread of projections from multiple members, which enables us to gain a better understanding of the uncertainties in climate modeling. The Hadley Centre has published 17 sets of boundary data from a perturbed physics ensemble (i.e., HadCM3Q0-Q16, known as QUMP), which is based on HadCM3 under the Special Report on Emissions Scenarios (SRES) A1B emission scenario, for use with PRECIS in order to allow users to generate an ensemble of high-resolution regional simulations (McSweeney and Jones 2010). Downscaling the 17-member PPE ensemble with PRECIS would require very large inputs of computing resources, data storage, and data analyses. To explore the range of uncertainties while minimizing these requirements, we select a subset of five members (i.e., HadCM3Q0, Q3, Q10, Q13, and Q15) from the QUMP ensemble according to the Hadley Centre's recommendation (see http://www.metoffice.gov.uk/precis/qump). HadCM3Q0 is first selected as it is the standard, unperturbed model using the original parameter settings as applied in the atmospheric component of HadCM3. Selection of the remaining four members is based on 1) their performances in simulating key features of the climate over Ontario, and 2) their ability to sample the range of outcomes of future changes simulated by the full 17-member ensemble (Bellprat et al. 2012).

We run five PRECIS experiments driven by boundary conditions from the selected GCM members from 1950 to 2099 at its highest horizontal resolution (i.e., 25 km). This allows us to carry out undermentioned probabilistic analyses by providing full simulation coverage from the present day to the future. The PRECIS model outputs are extracted and divided into four 30-yr periods: one baseline period (1961–90), and three future periods (2020–49, 2040–69, and 2070–99), representing its simulations for the province of Ontario under current and future climate forcings.

c. Data

We focus on the temperature responses over the province of Ontario under the SRES A1B emission scenario (Nakicenovic and Swart 2000). Three temperature-related variables, daily maximum temperature (Tmax), daily mean temperature (Tmean), and daily minimum temperature (Tmin), are extracted from the outputs of five PRECIS runs. Projection on each variable is divided into four 30-yr periods: 1961–90, 2020–49, 2040–69, and 2070–99. We regard the period of 1961–90 as a baseline so that the model outputs on this period can be used to represent simulation on current climate, while projections of future climate are reflected in the remaining three periods and simulation on each period will be separately treated. Observed temperature means for the baseline period are derived from the raster-gridded climate dataset provided by the National Land and Water Information Service, Agriculture and Agri-Food Canada. The dataset contains 10-km gridded point estimates of daily maximum temperature and minimum temperature, which are interpolated from daily Environment Canada climate station observations using a thin plate smoothing spline surface fitting method implemented by the ANUSPLIN V4.3 software package (NLWIS 2007). Daily mean temperature on each grid is calculated using (Tmax + Tmin)/2. The observed temperature means derived from the 10-km dataset are then regridded to the 25-km grids of PRECIS model.

3. Bayesian hierarchical model

Suppose we have observation data for the present climate, denoted as x_0, and the PRECIS simulations are expressed as x_i (for current climate) and y_i (for future climate), for $i = 1, 2, \ldots, N$; here $N = 5$, indicating the total number of PRECIS runs. We further assume that the PRECIS outputs depend on some parameters that are unknown due to uncertainties in climate models. In addition, the quality of observation data may be affected by some unexpected factors such as measurement error, equipment failure, and so on. Let Θ be the vector of all unknown parameters involved in both observations and model simulations. The Bayesian viewpoint allows us to treat these parameters as random variables in order to quantify the uncertainties of interest in a statistical way. Specifically, we can construct a probabilistic model for random parameters Θ, which are conditional to existing data D consisting of observations x_0 and model simulations x_i and y_i, as follows:

$$p(\Theta|D) \propto p(\Theta) \cdot p(D|\Theta), \tag{1}$$

where $p(\Theta|D)$ is the posterior distribution of Θ given our best understanding of the climate system based on existing observations and model simulations (it is a probabilistic representation of what we can conclude about the unknown parameters after we observe and model the climate system); $p(\Theta)$ is the prior distribution of Θ indicating what we know about the unknown parameters before we obtain data D; $p(D|\Theta)$ is the likelihood specifying the conditional distribution of the data given all involved parameters, which is formulated under some statistical assumptions; and the symbol $\propto$ means a proportional relationship up to a normalizing constant (namely marginal distribution), which is usually intractable integral and not necessary to compute in Markov chain Monte Carlo (MCMC) simulation (Brooks 1998). Therefore, an empirical estimate of the posterior distribution is usually obtained through a MCMC implementation to the statistical model, bypassing the need to compute it analytically. Statistical inferences can be drawn based on the MCMC samples using smoothed histograms, numerical analyses, etc.

a. Likelihoods

We assume Gaussian distribution for observations x_0:

$$x_0 \sim N(\mu, \lambda_0^{-1}), \tag{2}$$

where the notation $N(\mu, \lambda_0^{-1})$ indicates a Gaussian distribution with mean μ and variance λ_0^{-1}. Here μ represents the true value of current climate mean, and λ_0^{-1} is treated as a random variable to indicate that the observations are centered on the true value of current climate with a random error. Observations may suffer from both random errors (i.e., measurement and sampling) and systematic errors due to different measurement platforms and practices (Rayner et al. 2006). We use λ_0 here to account for these uncertainties in observations. Thus we express the statistical assumption for x_0 as follows:

$$x_0 = \mu + \chi, \tag{3}$$

where $\chi \sim N(0, \lambda_0^{-1})$.

Similarly, we assume Gaussian distribution for x_i:

$$x_i \sim N(\mu, \lambda_i^{-1}), \tag{4}$$

where λ_i is referred to as the precision of distributions x_i in estimating current climate, following the definition proposed by Tebaldi et al. (2005). The assumption underlying Eq. (4) is that the model simulation is a symmetric distribution, whose center is the true value of current climate, but with an individual variability. As such, λ_i can be treated as a quantity for assessing the performance of the ith PRECIS run in reproducing

current climate, while driven by the corresponding boundary conditions from the QUMP ensemble. Accordingly, the statistical assumption for x_i can be expressed as follows:

$$x_i = \mu + \eta_i, \tag{5}$$

where $\eta_i \sim N(0, \lambda_i^{-1})$. Projecting future climate with a climate model is to some extent correlated to its capability in hindcasting observed climate, so we therefore treat y_i and x_i as dependent distributions through a linear regression equation. Thus y_i can be formulated as follows:

$$y_i = \nu + \xi_i + \beta(x_i - \mu), \tag{6}$$

where ν represents the true value of future climate mean; $\xi_i \sim N[0, (\theta\lambda_i)^{-1}]$, the product of $\theta\lambda_i$ is referred to as the precision of distribution y_i in terms of simulating future climate, while θ is introduced as an additional parameter to allow for different precision for y_i from x_i in all PRECIS runs; and β is an unknown regression coefficient. A value of β equal to 0 indicates independence between y_i and x_i; otherwise, positive values imply direct relations and negative for inverse ones between these two quantities. Likewise, we assume the likelihood of y_i as a Gaussian distribution:

$$y_i \sim N[\nu + \beta(x_i - \mu), (\theta\lambda_i)^{-1}], \tag{7}$$

where we use the term of $\beta(x_i - \mu)$ to imply a linear adjustment to the projection of future climate based on the model bias for current climate simulation.

b. Prior distributions

The statistical model described by Eqs. (2), (4), and (7) are formulated using a set of parameters: $\{\mu, \nu, \beta, \theta, \lambda_0, \lambda_1, \ldots, \lambda_N\}$. We assume uninformative prior distributions for these parameters as follows:

(i) The true values of current and future climate means, μ and ν, are assumed to have uniform priors on the real line (i.e., $[-\infty, +\infty]$).

(ii) The regression coefficient (β) is presumed to be freely varying between -1 and $+1$, thus a uniform distribution on $[-1, 1]$.

(iii) Based on the estimation of Giorgi and Mearns (2002) in terms of natural variability of observed temperature at different regions for winter and summer seasons, we assume gamma prior density for λ_0 and the first guesses for its mean and variance are 4.5 and 19.3 respectively. Thus we formulate the prior distribution of λ_0 as follows:

$$\lambda_0 \sim \text{Gamma}(m, n) = \frac{n^m}{\Gamma(m)}\lambda_0^{m-1}e^{-n\lambda_0}, \tag{8}$$

where $m = 1.05$ and $n = 0.23$.

(iv) We assume gamma distributions for $\lambda_1, \ldots, \lambda_N$:

$$\lambda_i \sim \text{Gamma}(a, b) = \frac{b^a}{\Gamma(a)}\lambda_i^{a-1}e^{-b\lambda_i}, \quad i = 1, \ldots, N. \tag{9}$$

Similarly, gamma distribution for θ:

$$\theta \sim \text{Gamma}(c, d) = \frac{d^c}{\Gamma(c)}\theta^{c-1}e^{-d\theta}. \tag{10}$$

Here we set $a = b = c = d = 0.001$; this is to translate these assumed priors into gamma distributions with mean 1 and variance 1000 (Tebaldi et al. 2005). By doing so, we can get extremely diffused priors to reflect our poor understanding about these unknown parameters.

c. Posterior distributions

Inferences for the statistical model defined in Eq. (1) can be achieved by applying Bayesian theorem to the likelihoods and priors described above. The joint posterior distribution is obtained up to a constant by taking the product of all conditional distributions. Thus, we have

$$p(\Theta \mid D) \propto \prod_{i=1}^{N}\left[\lambda_i^{a-1}e^{-b\lambda_i}\cdot\lambda_i\sqrt{\theta}\,\exp\left(-\frac{\lambda_i}{2}\{(x_i-\mu)^2 + \theta[y_i - \nu - \beta(x_i-\mu)]^2\}\right)\right]$$
$$\cdot\,\theta^{c-1}e^{-d\theta}\cdot\lambda_0^{m-1}e^{-n\lambda_0}\cdot\sqrt{\lambda_0}\,\exp\left[-\frac{\lambda_0}{2}(x_0-\mu)^2\right]. \tag{11}$$

From Eq. (11) we can obtain full conditional distribution for each parameter by ignoring all other parameters that are constant with respect to the parameter of interest. In our case, full conditional distributions for all parameters are well-known distributions such as the gamma or Gaussian ones. We can therefore perform MCMC simulation through a Gibbs sampler. The formulation of the full conditional distributions for all parameters, the steps

TABLE 1. Twelve selected weather stations (UA denotes an upper air reporting station).

No.	Weather station	Longitude	Latitude	Abbreviation
001	Windsor Airport	82°96′W	42°28′N	WDA
002	London Int'l Airport	81°15′W	43°03′N	LIA
003	Toronto Lester B. Pearson Int'l Airport	79°63′W	43°68′N	TLA
004	Toronto City Center (Island Airport)	79°40′W	43°63′N	TCC
005	Ottawa Macdonald-Cartier Int'l Airport	75°67′W	45°32′N	OMA
006	Wiarton Airport	81°11′W	44°75′N	WTA
007	North Bay Airport	79°42′W	46°36′N	NBA
008	Sault Ste Marie Airport	84°51′W	46°48′N	SSA
009	Sioux Lookout Airport	91°90′W	50°12′N	SLA
010	Timmins Victor Power Airport	81°38′W	48°57′N	TVA
011	Big Trout Lake	89°87′W	53°83′N	BTL
012	Moosonee UA	80°65′W	51°27′N	MUA

of Gibbs sampler as well as the implementation of MCMC algorithm are given in appendixes A, B, and C.

Here we show how to obtain the probabilistic climate change projections based on the PRECIS experiments driven by different boundary conditions. First, the full conditional distribution of μ is derived from Eq. (11) by fixing all other parameters, as a Gaussian distribution:

$$p(\mu \mid x_0, x_1, \ldots, x_N, y_1, \ldots, y_N) \propto N\left\{ \frac{\sum_{i=1}^{N} [\lambda_i x_i - \theta\beta\lambda_i(y_i - \nu - \beta x_i)] + \lambda_0 x_0}{\lambda_0 + \sum_{i=1}^{N} \lambda_i(1 + \theta\beta^2)}, \left[\lambda_0 + \sum_{i=1}^{N} \lambda_i(1 + \theta\beta^2)\right]^{-1} \right\}. \quad (12)$$

In a similar way, the full conditional distribution of ν can be obtained as follows:

$$p(\nu \mid x_0, x_1, \ldots, x_N, y_1, \ldots, y_N) \propto N\left\{ \frac{\sum_{i=1}^{N} \lambda_i [y_i - \beta(x_i - \mu)]}{\sum_{i=1}^{N} \lambda_i}, \left(\theta \sum_{i=1}^{N} \lambda_i\right)^{-1} \right\}. \quad (13)$$

Likewise, we can derive the full conditional posterior distributions for the remaining parameters (as presented in appendix A). By doing a series of random drawings using Gibbs sampler, we have a large number of samples for μ and ν. The densities of these MCMC samples can be treated as approximate representations of their full conditional distributions. The climate change quantity is a random variable that can be represented by the difference between the true value of future climate and that of current climate, expressed as

$$\Delta = \nu - \mu. \quad (14)$$

Thus, the density of Δ can be estimated using the differences between two samples of ν and μ. Given the limited capability of climate models in representing the real climate system, we only can give plausible distribution for future climate change. We cannot say the absolute probability of climate changing by some exact values. Instead we talk about the probability of climate change being less than or greater than a certain value. Following the approach employed in the fifth generation of climate change information for the United Kingdom (UKCP09) (Murphy et al. 2009), we apply the cumulative distribution function (CDF) to define the probability of a climate change being less than or greater than a given amount, instead of using a probability density function (PDF). In particular, we use a cumulative probability of 90% to describe probabilistic projections by saying very likely to be less than or very unlikely to be greater than; we use a cumulative probability of 10% to indicate very likely to be greater than or very unlikely to be less than; and we define the value with a cumulative probability of 50% as the central estimate of projections (i.e., the median of the distribution). For convenience, we use the term probability level rather than cumulative probability hereinafter.

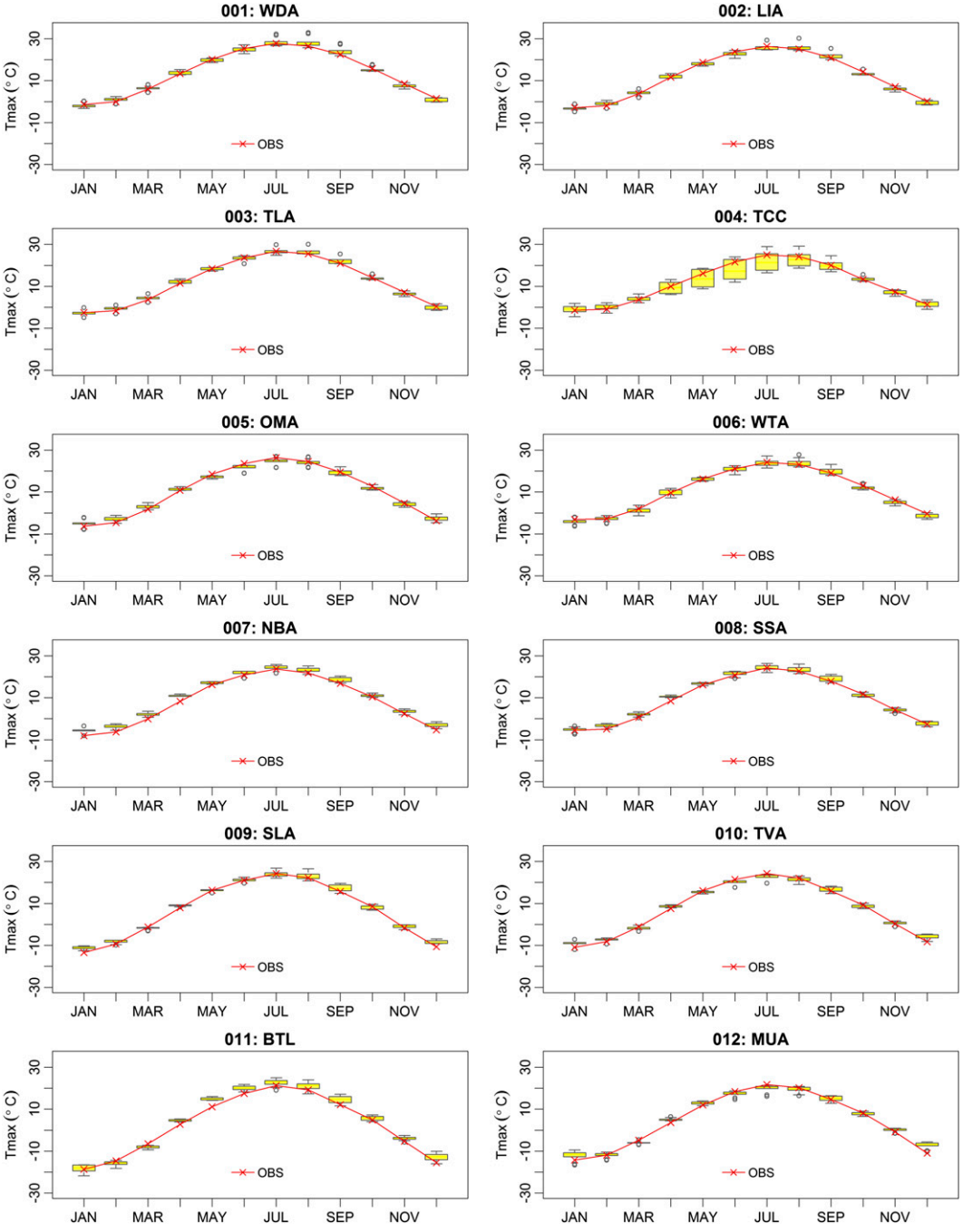

FIG. 2. Monthly means of Tmax at 12 weather stations.

4. Results

a. Capability of hindcasting current climate

As mentioned above, a five-member subset was screened out from the QUMP ensemble as boundary conditions to drive five individual PRECIS runs. To validate the capability of these five runs in simulating key features of current climate over Ontario, we choose 12 weather stations (see Table 1) from the weather and climate observing networks owned by Environment Canada to assess their overall performance. As shown in Fig. 1, these 12 stations are spatially distributed across the landmass of Ontario, allowing for capturing the spatial characteristics of model performance.

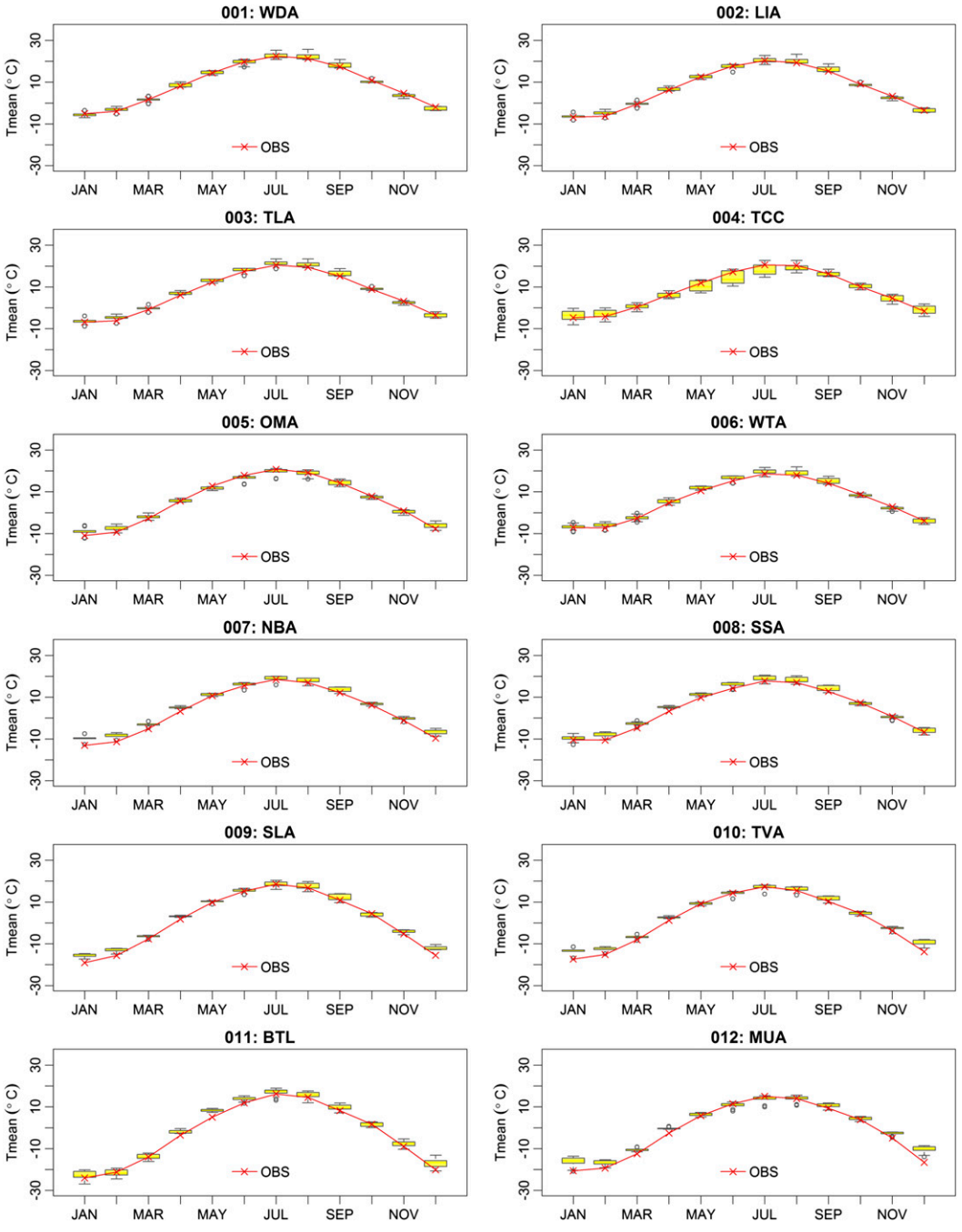

FIG. 3. Monthly means of Tmean at 12 weather stations.

Monthly temperature means for the baseline period at each weather station are calculated separately based on the outputs of five PRECIS runs. We then draw boxplots for monthly means of Tmax, Tmean, and Tmin separately at the 12 stations. Observed means are plotted over the corresponding boxplots to help us visually check if the observed climate is well simulated by the five-member ensemble.

Figures 2–4 show the boxplots for Tmax, Tmean, and Tmin respectively. Observed monthly means of Tmax and Tmean at 12 weather stations are well captured by the aggregated simulations from the ensemble runs. However, the ensemble simulations slightly overestimate Tmin in some weather stations located in the middle and northern areas. In particular, the observed means of Tmin at stations SLA, TVA, and MUA for winter

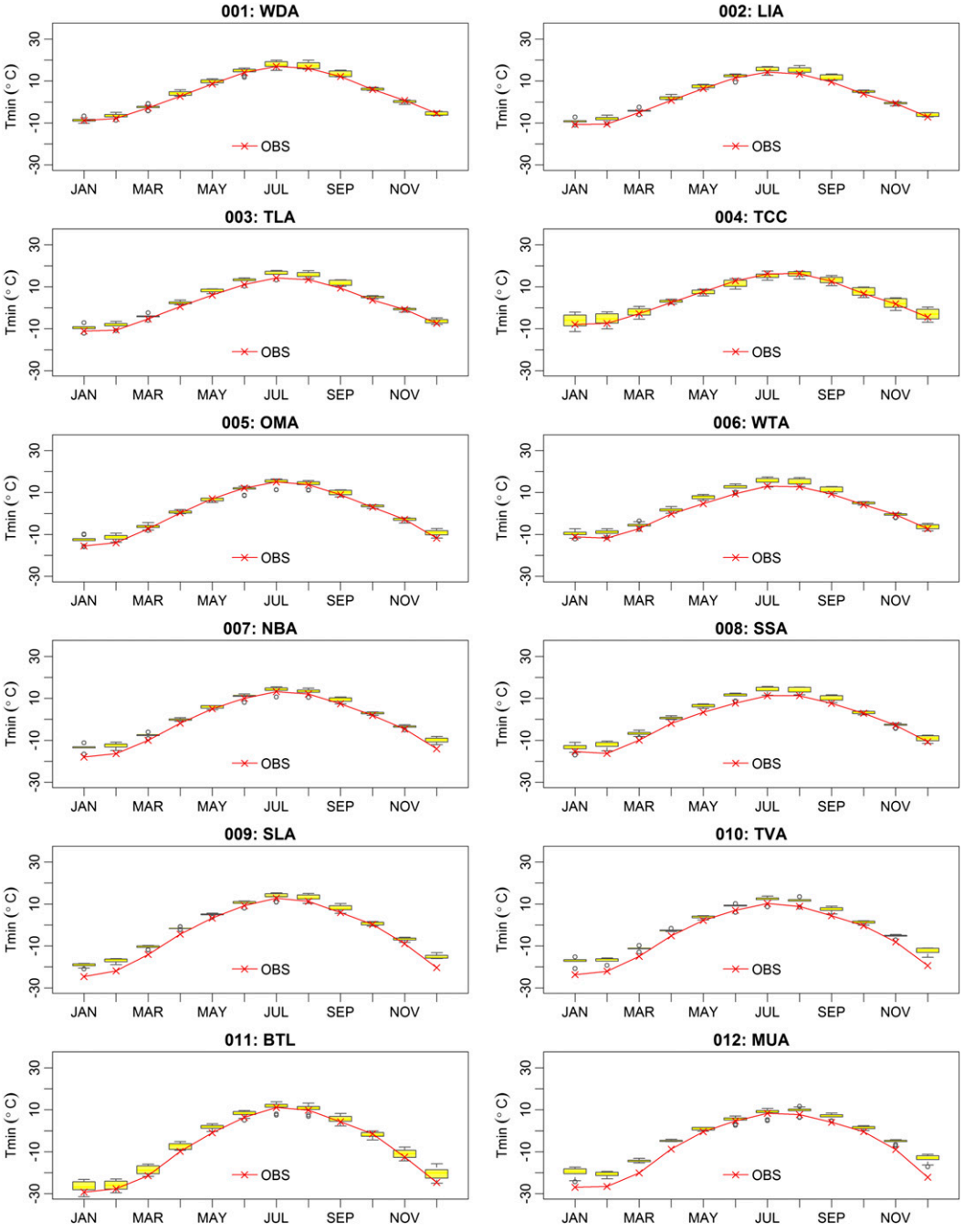

FIG. 4. Monthly means of Tmin at 12 weather stations.

(December–February) and spring (March–May) are less than the lower bound of simulated results. Otherwise, the observations are still fully covered by the interval bounded by the maximum and minimum values of five simulated values. Overall, the climate means and patterns over Ontario can be smoothly reflected by the PRECIS ensemble.

b. Posterior distributions at selected weather stations

By applying the Bayesian model, we derive posterior distributions for all random parameters based on the assumptions for the likelihoods and priors. Here we focus on analyzing the MCMC results of all parameters in terms of simulating three temperature variables

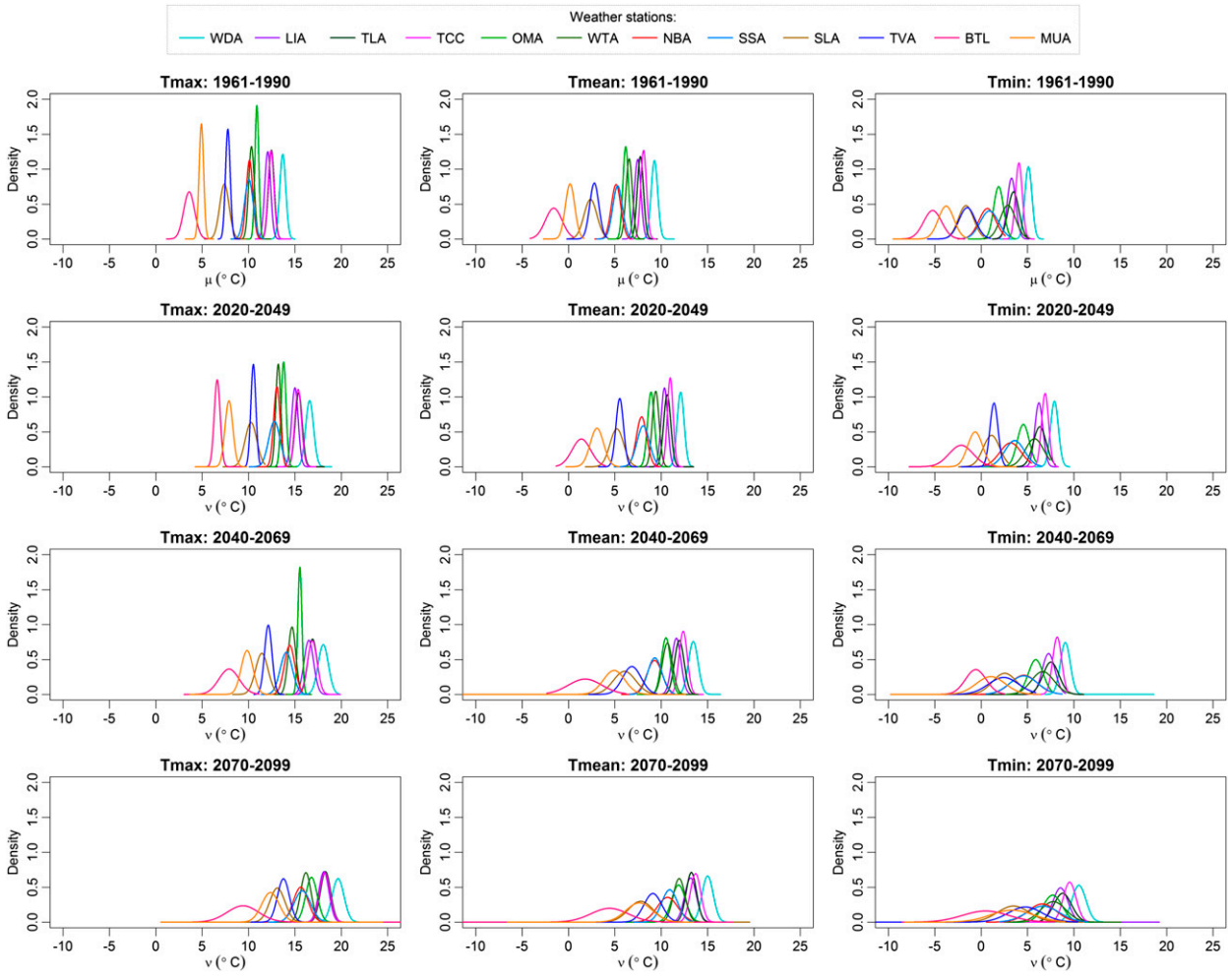

FIG. 5. Posterior distributions of μ (baseline period: 1961–90) and ν (three future periods: 2020–49, 2040–69, and 2070–99) for Tmax, Tmean, and Tmin at 12 weather stations.

(i.e., Tmax, Tmean, and Tmin) at the 12 weather stations under current and future climate forcings.

1) TEMPERATURE CHANGES

Figure 5 shows posterior distributions of μ and ν for Tmax, Tmean, and Tmin at 12 weather stations. In particular, we draw the density curves based on the MCMC samples for each temperature variable at each station. The true temperatures of present climate (i.e., μ) are estimated with the simulation for the baseline period, as illustrated by the top three plots. Likewise, simulate results for 2020–49, 2040–69, and 2070–99 are used to estimate the true values of future climate (i.e., ν), as shown in the remaining nine plots. Even though curves for 12 stations in each plot tell totally different stories, the means for Tmax, Tmean, and Tmin at all stations reveal consistently increasing trends throughout the twenty-first century.

To further analyze the temperature changes (i.e., $\Delta T = \nu - \mu$) under future climate, we extract the estimated values at three probability levels (i.e., 10%, 50%, and 90%) for Tmax, Tmean, and Tmin at 12 stations. Meanwhile, a 95% confidence interval (CI) is computed to give an estimation for the range of values that is likely to cover the possible changes under presumed uncertainties (Goldstein and Healy 1995). The results are listed in Table 2. Thus, we can interpret the temperature changes at each station with the corresponding confidence levels. For example, the Tmax change at station WDA for the period of 2020–49 is very likely to be greater than 2.64°C and is very likely to be less than 3.19°C, while the median change tends to be 2.92°C and the likely range for Tmax change would be [2.91, 2.93]°C for the same period; the Tmean change at station TCC under future climate of 2070–99 would be around 5.62°C and it is very likely to be greater than

TABLE 2. Projected temperature changes ($\Delta T = \nu - \mu$) at 12 weather stations.

Weather station	Probability level	Temperature variable								
		Tmax (°C)			Tmean (°C)			Tmin (°C)		
		2020–49	2040–69	2070–99	2020–49	2040–69	2070–99	2020–49	2040–69	2070–99
001: WDA	10%	2.64	3.92	5.4	2.58	3.84	5.17	2.56	3.64	4.84
	50%	2.92	4.32	5.99	2.81	4.17	5.68	2.79	3.99	5.42
	90%	3.19	4.75	6.61	3.09	4.53	6.17	3.01	4.35	6.02
	95% CI	[2.91, 2.93]	[4.31, 4.35]	[5.97, 6.03]	[2.81, 2.84]	[4.16, 4.2]	[5.65, 5.7]	[2.77, 2.79]	[3.98, 4.01]	[5.4, 5.45]
002: LIA	10%	2.64	4.06	5.53	2.62	3.86	5.24	2.58	3.63	4.86
	50%	2.94	4.41	6.05	2.86	4.18	5.73	2.83	4.01	5.37
	90%	3.24	4.79	6.58	3.12	4.52	6.19	3.05	4.38	5.92
	95% CI	[2.93, 2.95]	[4.4, 4.44]	[6.03, 6.08]	[2.85, 2.88]	[4.17, 4.2]	[5.7, 5.74]	[2.81, 2.84]	[3.99, 4.02]	[5.36, 5.4]
003: TLA	10%	2.68	4.04	5.47	2.63	3.87	5.16	2.53	3.53	4.82
	50%	2.97	4.38	5.87	2.86	4.18	5.57	2.79	4.03	5.36
	90%	3.24	4.71	6.29	3.1	4.5	5.96	3.03	4.55	5.9
	95% CI	[2.95, 2.97]	[4.36, 4.39]	[5.85, 5.89]	[2.85, 2.87]	[4.17, 4.2]	[5.55, 5.58]	[2.77, 2.8]	[4.01, 4.06]	[5.33, 5.39]
004: TCC	10%	2.69	4.04	5.4	2.64	4	5.22	2.64	3.83	4.98
	50%	2.95	4.4	5.82	2.86	4.26	5.62	2.83	4.11	5.47
	90%	3.2	4.76	6.26	3.08	4.55	6.02	3	4.37	5.98
	95% CI	[2.93, 2.96]	[4.38, 4.42]	[5.8, 5.85]	[2.85, 2.87]	[4.26, 4.28]	[5.6, 5.64]	[2.82, 2.83]	[4.09, 4.12]	[5.45, 5.5]
005: OMA	10%	2.73	4.42	5.36	2.58	3.94	5	2.48	3.65	4.91
	50%	2.92	4.59	5.91	2.78	4.29	5.7	2.72	4.1	5.74
	90%	3.09	4.76	6.5	2.97	4.61	6.33	2.95	4.54	6.53
	95% CI	[2.91, 2.92]	[4.58, 4.6]	[5.89, 5.94]	[2.77, 2.79]	[4.26, 4.3]	[5.65, 5.72]	[2.71, 2.73]	[4.07, 4.12]	[5.68, 5.76]
006: WTA	10%	2.63	4.15	5.42	2.62	3.77	5.02	2.28	3.14	4.34
	50%	2.86	4.4	5.87	2.82	4.1	5.46	2.68	3.78	5.08
	90%	3.1	4.65	6.29	3.01	4.43	5.86	3.04	4.4	5.77
	95% CI	[2.85, 2.87]	[4.38, 4.41]	[5.84, 5.88]	[2.81, 2.83]	[4.09, 4.12]	[5.43, 5.47]	[2.65, 2.69]	[3.75, 3.81]	[5.04, 5.1]
007: NBA	10%	2.73	3.94	5.1	2.53	3.67	4.82	2.24	3.27	4.69
	50%	2.88	4.31	5.64	2.75	4.11	5.6	2.63	4.01	5.67
	90%	3.02	4.63	6.18	2.96	4.59	6.34	3.04	4.71	6.64
	95% CI	[2.87, 2.88]	[4.28, 4.31]	[5.62, 5.67]	[2.73, 2.75]	[4.1, 4.14]	[5.56, 5.63]	[2.62, 2.65]	[3.97, 4.04]	[5.62, 5.72]
008: SSA	10%	2.49	3.67	5.11	2.51	3.66	5.09	2.37	3.22	4.69
	50%	2.74	4.1	5.69	2.76	4.06	5.54	2.7	3.95	5.6
	90%	2.99	4.5	6.26	3.01	4.5	6	3.05	4.64	6.45
	95% CI	[2.73, 2.75]	[4.08, 4.12]	[5.67, 5.72]	[2.75, 2.77]	[4.05, 4.09]	[5.53, 5.57]	[2.69, 2.73]	[3.91, 3.98]	[5.54, 5.63]
009: SLA	10%	2.48	3.67	5.05	2.39	3.1	4.57	2.31	3.28	4.22
	50%	2.69	4.08	5.78	2.66	3.84	5.44	2.63	4.01	5.38
	90%	2.9	4.47	6.56	2.96	4.51	6.35	2.97	4.72	6.58
	95% CI	[2.68, 2.7]	[4.05, 4.09]	[5.76, 5.83]	[2.65, 2.68]	[3.78, 3.85]	[5.41, 5.49]	[2.62, 2.65]	[3.97, 4.04]	[5.34, 5.45]
010: TVA	10%	2.71	4.09	5.43	2.57	3.61	5.36	2.51	3.33	4.82
	50%	2.8	4.35	5.97	2.77	4.2	6.11	2.78	4.19	6.08
	90%	2.89	4.61	6.51	2.98	4.77	6.93	3.05	5.03	7.33
	95% CI	[2.8, 2.8]	[4.34, 4.36]	[5.95, 6]	[2.76, 2.78]	[4.17, 4.22]	[6.08, 6.16]	[2.77, 2.79]	[4.15, 4.22]	[6.02, 6.14]

TABLE 2. (*Continued*)

Weather station	Probability level	Temperature variable								
		Tmax (°C)			Tmean (°C)			Tmin (°C)		
		2020–49	2040–69	2070–99	2020–49	2040–69	2070–99	2020–49	2040–69	2070–99
011: BTL	10%	2.78	3.63	4.61	2.37	2.56	4.43	2.45	3.75	4.2
	50%	2.92	4.37	5.83	2.79	3.72	5.93	2.94	4.51	5.97
	90%	3.05	5.06	7.16	3.19	4.88	7.36	3.51	5.2	7.76
	95% CI	[2.91, 2.92]	[4.32, 4.39]	[5.79, 5.91]	[2.77, 2.81]	[3.66, 3.77]	[5.85, 5.99]	[2.93, 2.98]	[4.46, 4.53]	[5.9, 6.07]
012: MUA	10%	2.61	4.28	6.18	2.47	3.7	5.69	2.5	3.72	5.33
	50%	3.03	4.99	7.36	2.98	4.76	7.21	3.04	4.87	7.23
	90%	3.43	5.67	8.42	3.53	5.89	8.8	3.56	5.95	9
	95% CI	[3.01, 3.05]	[4.95, 5.02]	[7.28, 7.39]	[2.96, 3.01]	[4.73, 4.83]	[7.16, 7.3]	[3.01, 3.06]	[4.8, 4.91]	[7.13, 7.31]

5.22°C and less than 6.02°C, while the credible estimate of changing interval would be [5.60, 5.64]°C. The results also report a gradient increase with time to the change of each temperature index at each weather station. For example, the median values of Tmean change at all stations range from 2.66°C (at SLA) to 2.98°C (at MUA) for the period of 2020–49; the range of these values for the period of 2040–69 would rise up to [3.72, 4.76]°C, with the lower bound at BTL and the upper one at MUA; to the end of the twenty-first century, the change of Tmean would jump to as high as 7.21°C at MUA, with the least change being 5.44°C at SLA.

2) MODEL RELIABILITY AND INFLATION-DEFLATION EFFECTS

We use λ_i to reflect the precision of each PRECIS model run in terms of reproducing the current observed climate, while an inflation/deflation parameter (θ) is introduced to represent its performance in simulating climate under future forcing, with the form of $\theta\lambda_i$. Figures 6 and 7 present the posterior distributions for λ_i and θ in the form of box plots, with logarithmically scaled horizontal axes because of their high degree of skewness (Tebaldi et al. 2005). In our analysis, λ_i is used as a scoring criterion to evaluate the overall performance of each PRECIS run in terms of simulating current climate forcing. It will be further treated as a weighting coefficient to reflect the contribution of each model run to the final combined estimate. However, λ_i here is a random variable with gamma posterior distribution; the scoring of five PRECIS runs should be assessed through the relative positions of the box plots at 12 stations, rather than by comparing point estimates. To facilitate our analysis, we draw a vertical line at 1 for each box plot in Fig. 6, which is helpful to compare the overall performance of all model runs. Specifically, we use the location of the median line within a box plot relative to line 1 to represent its relative position. Evaluating the overall performance of a model run may suggest a complete consideration of its individual precisions in reproducing the current climate conditions of 12 weather stations. For example, a model with box plots mostly distributed to the right side of 1 receives a higher score than the one with left-distributed box plots gains. Thus, we can rank the precisions of five PRECIS runs by computing the proportion of stations with box plots shifted to the right (shown in Table 3). For the run driven by HadCM3Q0, the proportions for Tmax, Tmean, and Tmin are all as high as 100%, which leads to the highest rank in its overall performance. By contrast, the run driven by HadCM3Q3

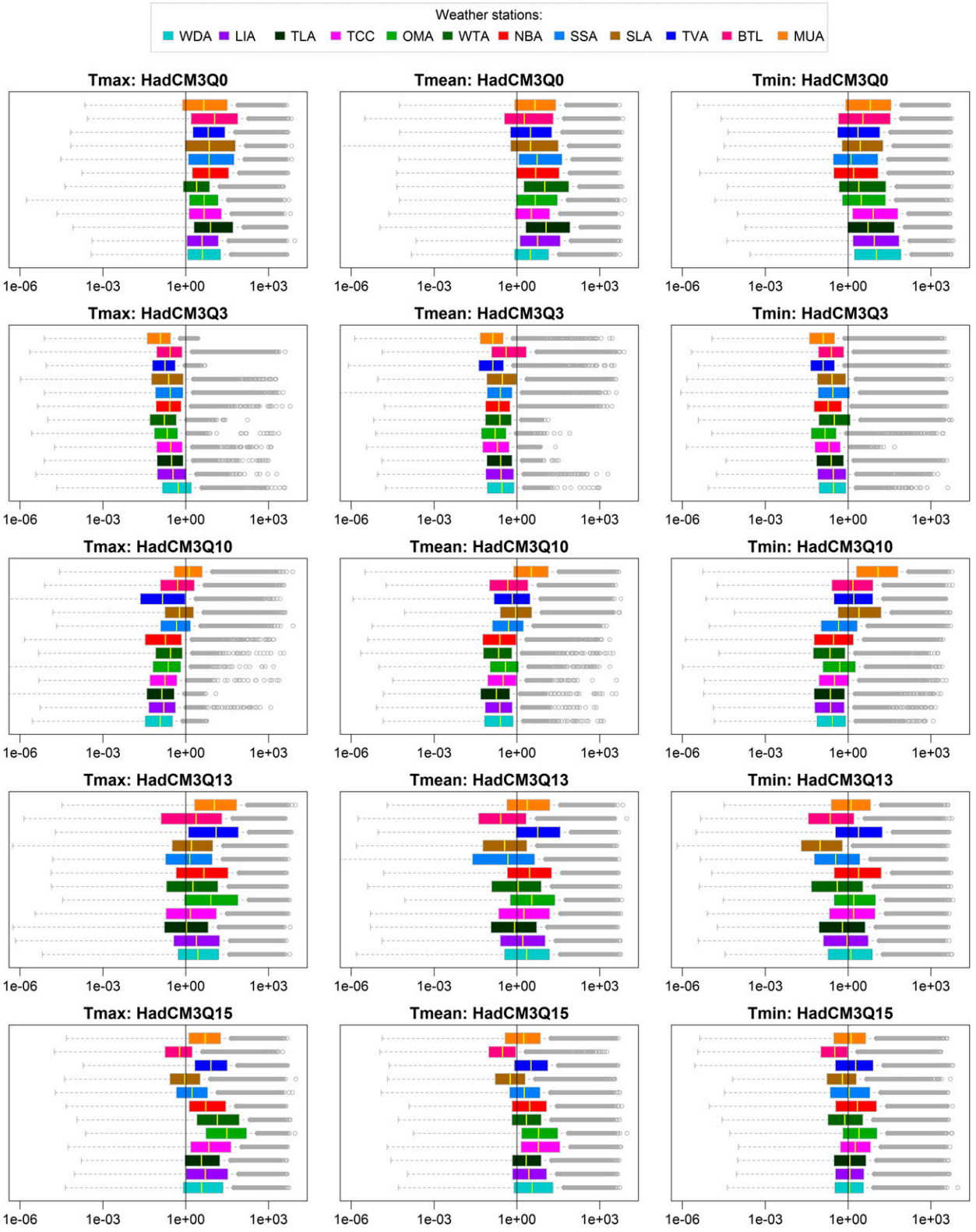

FIG. 6. Posterior distributions of λ_i at 12 stations. The three plots in the first row show the posterior distributions of λ_1 for Tmax, Tmean, and Tmin, respectively, where the PRECIS is driven by the boundary conditions of HadCM3Q0. Similarly, the remaining four rows contain box plots for λ_2, λ_3, λ_4, and λ_5, which are driven by HadCM3Q3, Q10, Q13, and Q15, respectively.

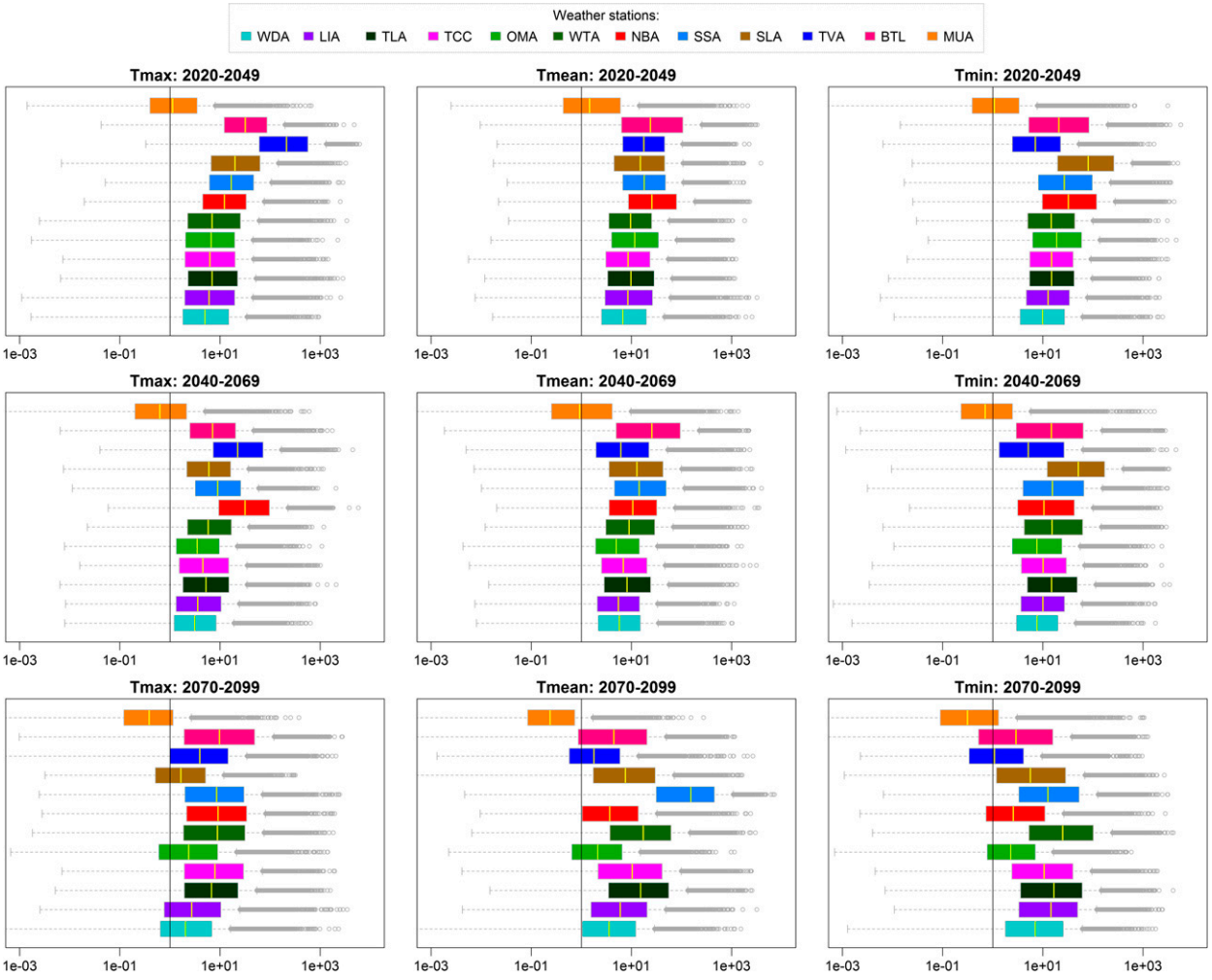

FIG. 7. Posterior distributions of θ at 12 stations for three future periods. For reference, we draw a vertical line at 1 to assess the consistency of PRECIS model precision between control simulation and future simulation.

gains the lowest rank because all box plots are distributed in the left side of 1. Among the remaining three runs, the ones driven by HadCM3Q15 and Q13 are both well rated owing to their good performance in more than half the stations (ranking second and third respectively), whereas the one driven by HadCM3Q10 performs relatively poorly (ranking the fourth) in the majority of the 12 weather stations.

The inflation/deflation parameter (θ) is useful to help understand if a well-performed model run in the

TABLE 3. Overall performance of five PRECIS runs. The model with a higher rank shows better performance than the one with a lower rank.

PRECIS run ID	GCM boundary condition	Proportion of stations with right-distributed box plots			Rank of overall performance
		Tmax	Tmean	Tmin	
regaa	HadCM3Q0	100%	100%	100%	1
regab	HadCM3Q3	0%	0%	0%	5
regac	HadCM3Q10	8.3%	8.3%	33.3%	4
regad	HadCM3Q13	91.7%	66.7%	50%	3
regae	HadCM3Q15	83.3%	83.3%	66.7%	2

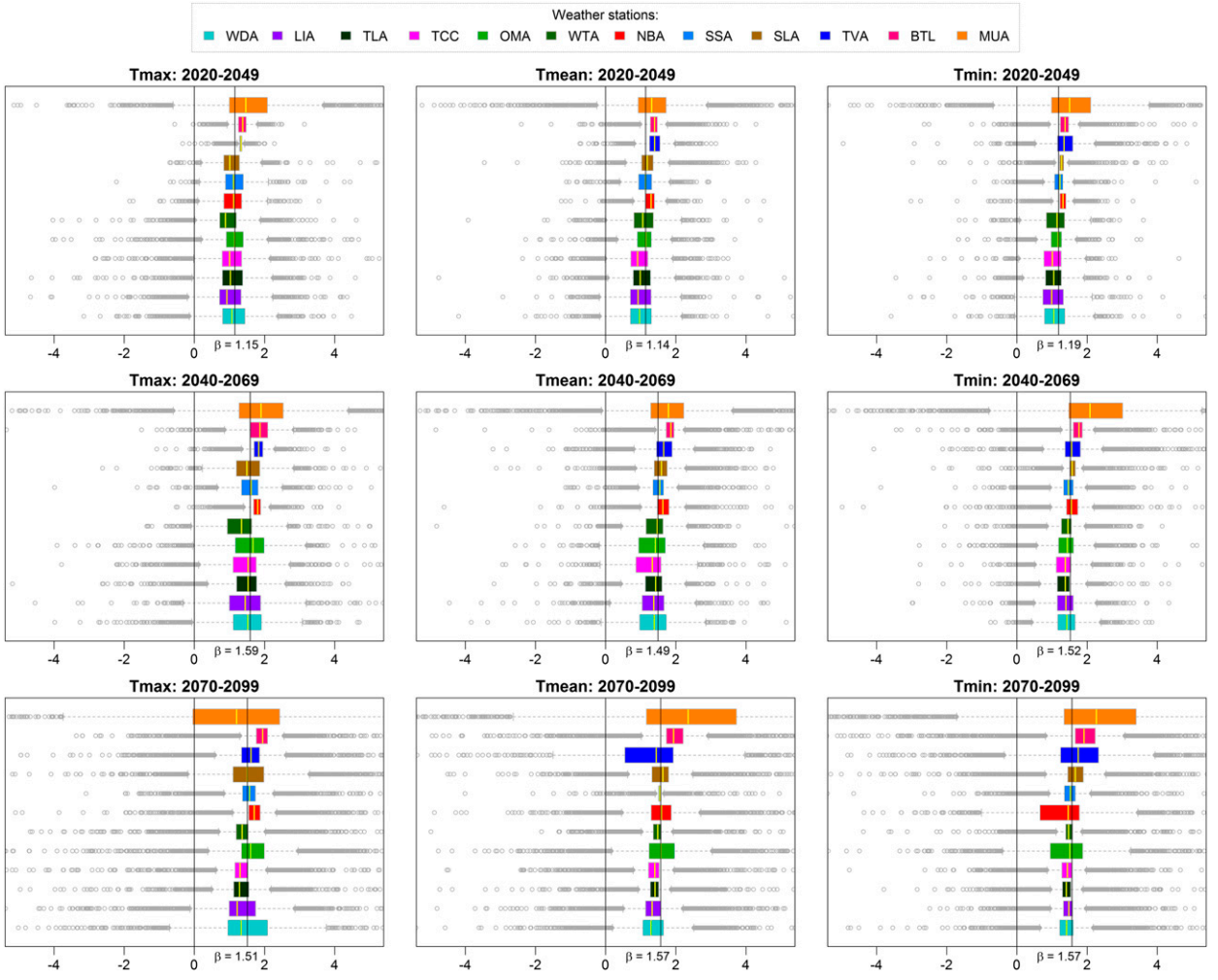

FIG. 8. Posterior distribution of β at 12 stations for three future periods. For reference, we draw a vertical line at 0 to help assess the significance of correlation between y_i and x_i, and a vertical line at the mean of 12 median values in each plot to assess the significance of the parameter magnitude.

control simulation period would behave similarly or inversely in the future climate simulation. Figure 7 indicates that almost all of the weather stations report varying levels of inflation in simulating the three temperature variables, with an average inflation factor on the order of 10. It is very interesting to realize that station MUA is the only exception, oppositely expressing a deflation behavior in the periods of 2040–69 and 2070–99. However, the deflation of this individual station is not likely to squash or offset the overall magnifying trend. The consistence of inflated performance in eleven-twelfths of weather stations may imply that the PRECIS model would project future climate with higher precision than it does in the current climate simulation. But this implication is conditional on our single-model ensemble runs driven by the boundary conditions from HadCM3; further exploration in terms of such inflation or deflation effects can be done by combining different RCMs and GCMs (Hewitt 2004; Kendon et al. 2010; Mearns et al. 2009, 2012).

3) TEMPORAL CORRELATION

By introducing parameter β in the Bayesian model, we are able to investigate the degree of correlation of the model simulations between future climate (y_i) and current climate (x_i). Figure 8 shows the distributions of β at 12 weather stations for three temperature variables and three future 30-yr periods, in the form of box plots. It is noticeable that most of the mass of the posterior densities is shifted in the right side of 0, with the mean of median values concentrated around 1.4. This implies a strong positive correlation between future climate

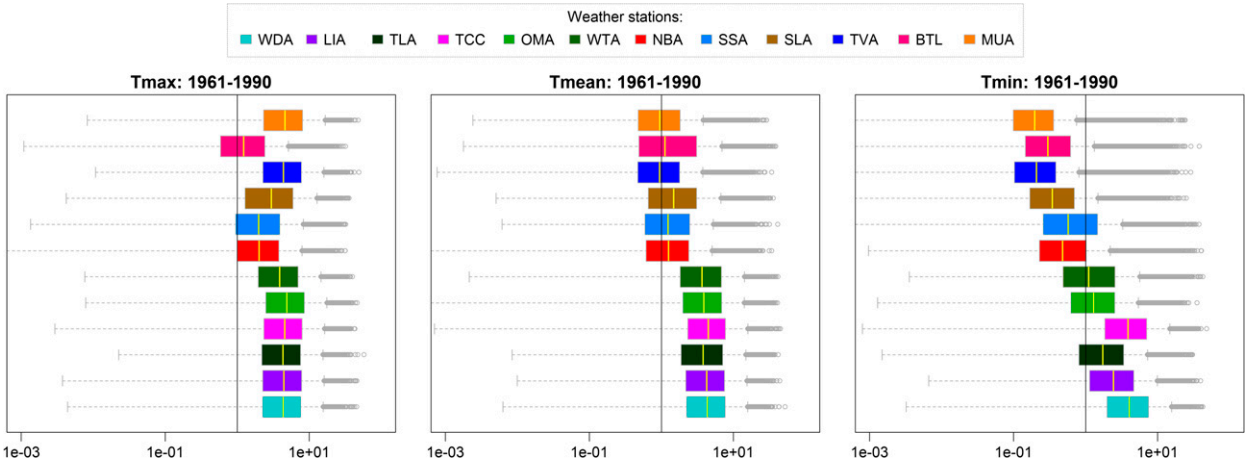

FIG. 9. Posterior distribution of λ_0 at 12 stations. For reference, we draw a vertical line at 1 to help assess the significance of the parameter magnitude.

projections and controlled climate simulation in each PRECIS experiment.

4) OBSERVATIONAL ERRORS

Figure 9 shows the posterior densities of λ_0, which is introduced here to quantify the uncertainties in observational data owing to system errors or natural variability, at 12 stations for three temperature variables. Similarly, we apply a logarithmically scaled axis in the box plots to help understand how the mass of the posterior densities is distributed. The plots for Tmax, Tmean, and Tmin show different patterns at 12 stations, but there is a common left-shifting tendency from Tmax to Tmean, then to Tmin while we compare the mass distributions for these three variables one station by one. Since λ_0^{-1} is referred to as the variance of observational data, bigger λ_0 suggests smaller variance and better quality of the observed data used in our analysis. Thus, these posterior distributions of λ_0 may give some insights into the quality of observational data. For example, the observation for Tmax used in this study is more likely to be concentrated on the true value of current climate with smaller deviation than the observed Tmin.

c. *Maps of projected temperature changes*

The purpose of this section is to display a number of maps to help understand the geographical patterns of temperature changes across the domain of Ontario at different probability levels. We calculates the changes of three temperature variables at nine probability levels (i.e., 10%, 20%, ... , 90%) offline (the results can be downloaded from http://env.uregina.ca/moe/pdownload/). We here show the changes at 10%, 50%, and 90% probability levels. The maps are at 25-km resolution covering the landmass and all water areas over Ontario.

Figure 10 shows the projected changes of Tmax at different probability levels. The central estimates of change are projected to increase significantly with time periods, and so are the changes at 10% and 90% probability levels. Specifically, in the period of 2020–49, the central estimates of change are projected to be generally between 2° and 3°C across most of the province, with slightly larger changes in the northeast next to the James Bay. The changes of Tmax at 50% probability level in 2040–69 would go up to [4, 5]°C in most of the domain. Furthermore, the projected central estimates of change in 2070–99 would be as high as [6, 8]°C in the northeast, with slightly smaller changes between 5° and 6°C in the southeast and the west of Ontario. It seems that the projected changes are very unlikely to be less than 2°C (in 2020–49) and very unlikely to be greater than 10°C (in 2070–99).

The changes of Tmin, as shown in Fig. 11, reveal similar patterns as those of Tmax, but with relatively smaller magnitudes compared to the changes of Tmax. The central estimates of changes in mean daily minimum temperature are projected to be [2, 3]°C in 2020–49, [4, 5]°C in 2040–69, and [5, 7]°C in 2070–99, respectively. The changes in Tmin are very unlikely to be less than 1°C (in 2020–49) and very unlikely to be greater than 10°C (in 2070–99).

Figure 12 shows that, as with Tmax and Tmin, there is a temporally gradient increase in terms of changing magnitudes of daily mean temperature from 2020–49 to 2070–99. In addition, each map shows a gradient

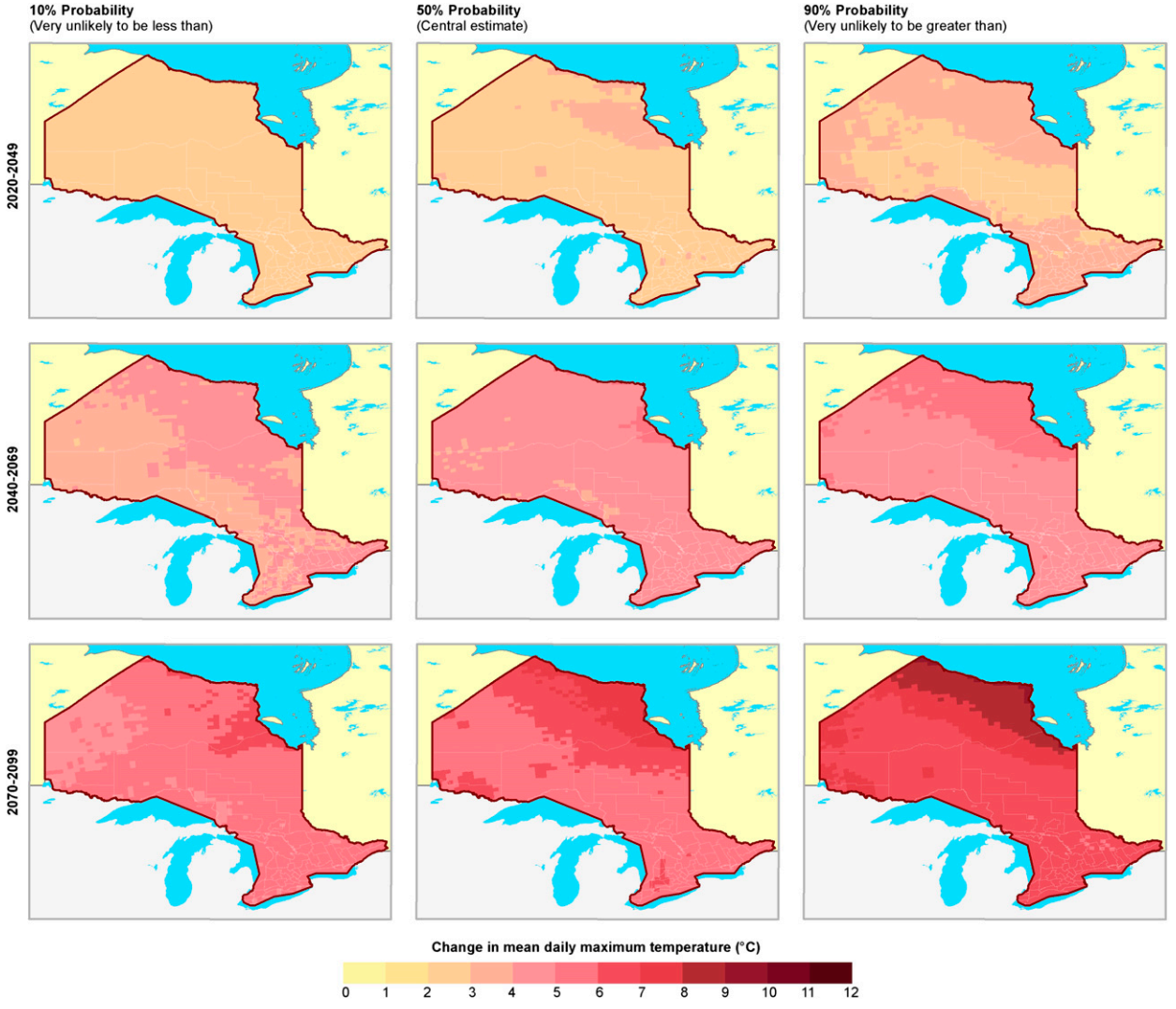

FIG. 10. Tmax changes at 10%, 50%, and 90% probability levels.

decreasing pattern for Tmean changes from the northeast, where the central estimates of changes in Tmean can be as high as 8°C in 2070–99, to the southwest, where the projected changes in the same period at 50% probability level can be 6°C or less. Such a spatially distributed pattern may be somewhat related to the large water bodies (i.e., Hudson Bay and James Bay) surrounding most parts of northern Ontario.

5. Summary and conclusions

In this study, we developed a high-resolution RCM ensemble for the province of Ontario, Canada, by using a subset of 17-member PPE ensemble from HadCM3 as boundary conditions to drive the PRECIS regional modeling system from 1950 to 2099. An advancement to the method proposed by Tebaldi et al. (2005) was presented to facilitate the calculation of the probabilities of temperature changes at grid point scale. The advanced method treated the unknown quantities of interest, such as observational errors, model reliability, and temporal correlation, as well as true climate signals, as random variables with uninformative prior distributions. A Bayesian hierarchical model was employed to quantify the uncertainties of these quantities in a statistical framework based upon a limited number of explicit assumptions. By feeding the observations for current climate and simulations from the RCM ensemble into the Bayesian model, we obtained posterior distributions of all the uncertain quantities of interest through MCMC simulations.

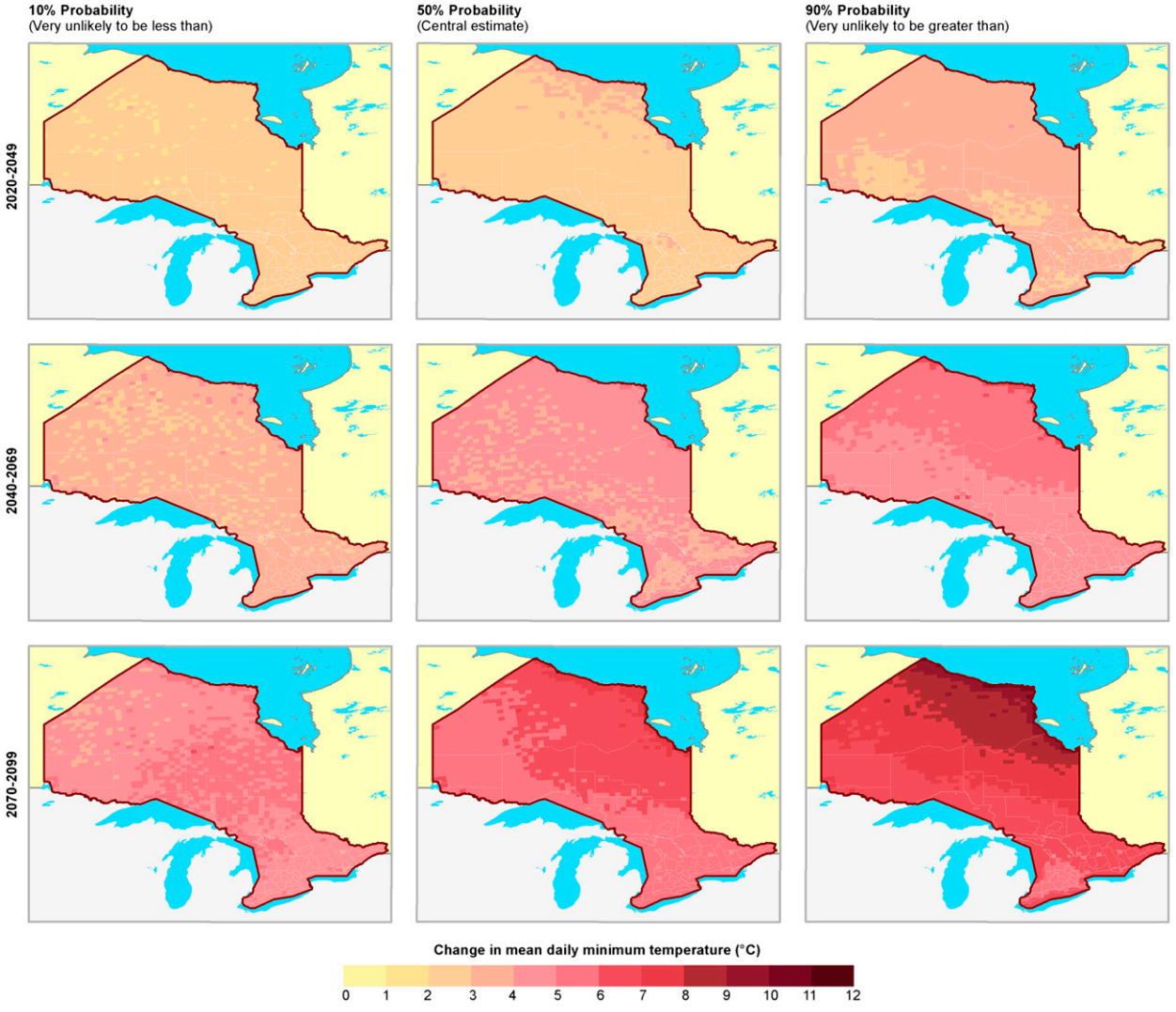

FIG. 11. Tmin changes at 10%, 50%, and 90% probability levels.

Following that, we computed the probabilities of changes in Tmax, Tmean, and Tmin at ~1800 25-km grids for three 30-yr periods: 2020–49, 2040–69, and 2070–99. Posterior distributions for all uncertain parameters at 12 selected weather stations were derived and analyzed in detail to investigate the practical significance of the proposed statistical model. We then presented maps of projected temperature changes at different probability levels to help understand the spatial patterns across the entire province.

The results show that there is likely to be a significant warming trend throughout the twenty-first century over Ontario. The central estimate of change in mean temperature in 2020–49 would be 2°–4°C, but this value is likely to increase dramatically in future time periods (3°–5°C in 2040–69, and 5°–8°C in 2070–99). The maps for Tmax and Tmin reveal the similar temporally increasing trends in terms of the magnitude of change from 2020–49 to 2070–99. In addition, there is obviously a spatially gradient decrease in the changes of three temperature variables from the northeast (with higher changes) to the southwest (with lower ones). The probabilistic projections suggest that people in Ontario are very unlikely to suffer a change less than 2°C to mean temperature in the forthcoming decades and very unlikely to suffer a change greater than 10°C to the end of this century.

The Bayesian hierarchical model presented here is not restricted to the high-resolution PRECIS ensemble developed for the province of Ontario. It can be applied directly to other GCM or RCM

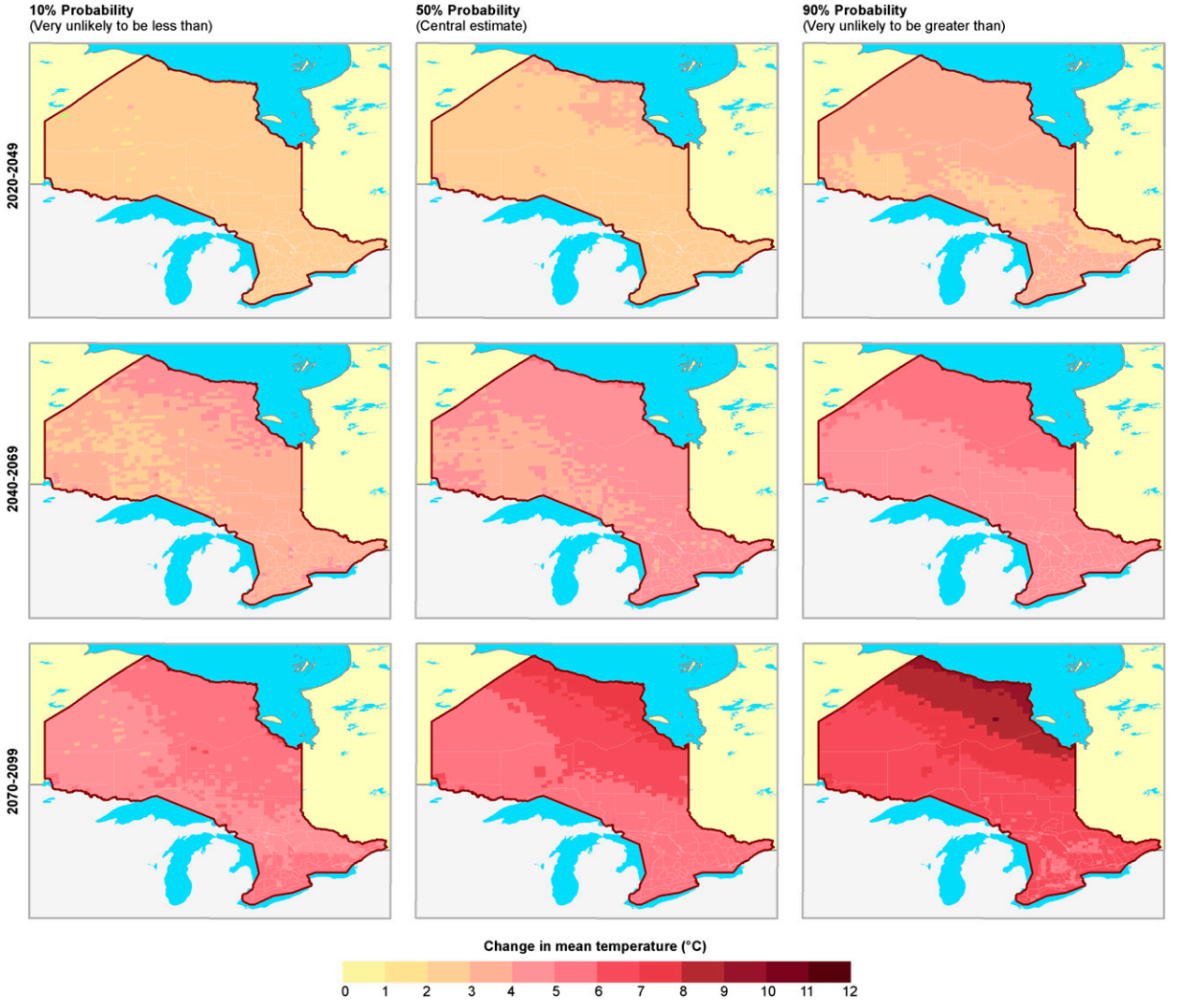

FIG. 12. Tmean changes at 10%, 50%, and 90% probability levels.

ensembles to construct more reliable projections for future climate change by quantifying related uncertainties in a statistical framework, and thus to provide useful information for assessing the risks and costs associated with climatic changes at global and regional scales.

Acknowledgments. This research was supported by the Major Project Program of the Natural Sciences Foundation (51190095), the Program for Innovative Research Team in University (IRT1127), Ontario Ministry of Environment and the Natural Science and Engineering Research Council of Canada.

APPENDIX A

Bayesian Model Formulation

1) Likelihoods for existing data x_0, x_i, y_i:

$$x_0 \sim N(\mu, \lambda_0^{-1}) = \frac{\sqrt{\lambda_0}}{\sqrt{2\pi}} \exp\left[-\frac{\lambda_0 (x_0 - \mu)^2}{2}\right]$$

$$x_i \sim N(\mu, \lambda_i^{-1}) = \frac{\sqrt{\lambda_i}}{\sqrt{2\pi}} \exp\left[-\frac{\lambda_i (x_i - \mu)^2}{2}\right]$$

$$y_i \sim N[\nu + \beta(x_i - \mu), (\theta\lambda_i)^{-1}] = \frac{\sqrt{\theta\lambda_i}}{\sqrt{2\pi}} \exp\left\{-\frac{\theta\lambda_i [y_i - \nu - \beta(x_i - \mu)]^2}{2}\right\}$$

2) Prior distributions for parameters μ, ν, β, θ, λ_0, λ_1, $\ldots$, λ_N:

Assume uniform prior densities on the real line for μ and ν, uniform prior distribution on $[-1, 1]$ for β, respectively. For the remaining parameters, we assume gamma distributions as follows:

$$\lambda_0 \sim \text{Gamma}(m, n) = \frac{n^m}{\Gamma(m)} \lambda_0^{m-1} e^{-n\lambda_0}$$

$$\lambda_i \sim \text{Gamma}(a, b) = \frac{b^a}{\Gamma(a)} \lambda_i^{a-1} e^{-b\lambda_i}, \quad i = 1, \ldots, N$$

$$\theta \sim \text{Gamma}(c, d) = \frac{d^c}{\Gamma(c)} \theta^{c-1} e^{-d\theta}$$

3) Posterior is given by, up to a normalizing constant,

$$\begin{aligned} p(\Theta \mid D) &= p(\mu, \nu, \beta, \theta, \lambda_0, \lambda_1, \ldots, \lambda_N \mid x_0, x_1, \ldots, x_N, y_1, \ldots, y_N) \\ &\propto p(\mu) \cdot p(\nu) \cdot p(\beta) \cdot p(\theta) \cdot p(\lambda_0) \cdot \prod_{i=1}^{N} p(\lambda_i) \cdot p(x_0 \mid \mu, \lambda_0) \cdot \prod_{i=1}^{N} p(x_i \mid \mu, \lambda_i) \cdot \prod_{i=1}^{N} p(y_i \mid \upsilon, \theta, \lambda_i, \beta, x_i, \mu) \\ &\propto \prod_{i=1}^{N} \left[\lambda_i^{a-1} e^{-b\lambda_i} \cdot \lambda_i \sqrt{\theta} \exp\left(-\frac{\lambda_i}{2}\{(x_i - \mu)^2 + \theta[y_i - \nu - \beta(x_i - \mu)]^2\}\right)\right] \\ &\cdot \theta^{c-1} e^{-d\theta} \cdot \lambda_0^{m-1} e^{-n\lambda_0} \cdot \sqrt{\lambda_0} \exp\left[-\frac{\lambda_0}{2}(x_0 - \mu)^2\right] \end{aligned}$$

Thus, we can obtain full conditional distributions for each parameter by ignoring all terms that are constant with respect to the parameter:

Full conditional for θ:

$$\begin{aligned} &p(\theta \mid \mu, \nu, \beta, \lambda_0, \lambda_1, \ldots, \lambda_N, x_0, x_1, \ldots, x_N, y_1, \ldots, y_N) \\ &\propto \prod_{i=1}^{N} \left[\sqrt{\theta} \exp\left\{-\frac{1}{2}\theta\lambda_i [y_i - \nu - \beta(x_i - \mu)]^2\right\}\right] \theta^{c-1} e^{-d\theta} \\ &\propto \theta^{(c+N/2)-1} \exp\left(-\theta\left\{d + \frac{1}{2}\sum_{i=1}^{N} \lambda_i [y_i - \nu - \beta(x_i - \mu)]^2\right\}\right) \\ &\propto \text{Gamma}\left\{c + \frac{N}{2}, d + \frac{1}{2}\sum_{i=1}^{N} \lambda_i [y_i - \nu - \beta(x_i - \mu)]^2\right\} \end{aligned}$$

Full conditional for β:

$$
\begin{aligned}
&p(\beta \mid \mu, \nu, \theta, \lambda_0, \lambda_1, \ldots, \lambda_N, x_0, x_1, \ldots, x_N, y_1, \ldots, y_N) \\
&\quad \propto \prod_{i=1}^{N} \exp\left\{-\frac{1}{2}\theta\lambda_i[y_i - \nu - \beta(x_i - \mu)]^2\right\} \\
&\quad \propto \exp\left\{-\frac{1}{2}\theta\left[\beta^2 \sum_{i=1}^{N} \lambda_i (x_i - \mu)^2 - 2\beta \sum_{i=1}^{N} \lambda_i (y_i - \nu)(x_i - \mu)\right]\right\} \\
&\quad \propto \exp\left\{-\frac{1}{2}\theta \sum_{i=1}^{N} \lambda_i (x_i - \mu)^2 \left[\beta - \frac{\sum_{i=1}^{N} \lambda_i (y_i - \nu)(x_i - \mu)}{\sum_{i=1}^{N} \lambda_i (x_i - \mu)^2}\right]^2\right\} \\
&\quad \propto N\left\{\frac{\sum_{i=1}^{N} \lambda_i (y_i - \nu)(x_i - \mu)}{\sum_{i=1}^{N} \lambda_i (x_i - \mu)^2}, \left[\theta \sum_{i=1}^{N} \lambda_i (x_i - \mu)^2\right]^{-1}\right\}
\end{aligned}
$$

Full conditional for λ_0:

$$
\begin{aligned}
&p(\lambda_0 \mid \mu, \nu, \beta, \theta, \lambda_1, \ldots, \lambda_N, x_0, x_1, \ldots, x_N, y_1, \ldots, y_N) \\
&\quad \propto (\lambda_0^{m-1} e^{-n\lambda_0}) \sqrt{\lambda_0} \exp\left[-\frac{\lambda_0}{2}(x_0 - \mu)^2\right] \\
&\quad \propto \lambda_0^{(m+1/2)-1} \exp\left\{-\lambda_0\left[n + \frac{1}{2}(x_0 - \mu)^2\right]\right\} \\
&\quad \propto \text{Gamma}\left[m + \frac{1}{2}, n + \frac{1}{2}(x_0 - \mu)^2\right]
\end{aligned}
$$

Full conditional for λ_i, $i = 1, \ldots, N$:

$$
\begin{aligned}
&p(\lambda_i \mid \mu, \nu, \beta, \theta, \lambda_0, \lambda_1, \ldots, \lambda_{i-1}, \lambda_{i+1}, \ldots, \lambda_N, x_0, x_1, \ldots, x_N, y_1, \ldots, y_N) \\
&\quad \propto (\lambda_i^{a-1} e^{-b\lambda_i}) \lambda_i \sqrt{\theta} \exp\left(-\frac{\lambda_i}{2}\{(x_i - \mu)^2 + \theta[y_i - \nu - \beta(x_i - \mu)]^2\}\right) \\
&\quad \propto \lambda_i^{(a+1)-1} \exp\left[-\lambda_i\left(b + \frac{1}{2}\{(x_i - \mu)^2 + \theta[y_i - \nu - \beta(x_i - \mu)]^2\}\right)\right] \\
&\quad \propto \text{Gamma}\left(a + 1, b + \frac{1}{2}\{(x_i - \mu)^2 + \theta[y_i - \nu - \beta(x_i - \mu)]^2\}\right)
\end{aligned}
$$

Full conditional for μ:

$$
\begin{aligned}
&p(\mu \mid \nu, \beta, \theta, \lambda_0, \lambda_1, \ldots, \lambda_N, x_0, x_1, \ldots, x_N, y_1, \ldots, y_N) \\
&\quad \propto \prod_{i=1}^{N} \left[\exp\left(-\frac{\lambda_i}{2} \{(x_i - \mu)^2 + \theta[y_i - \nu - \beta(x_i - \mu)]^2\} \right) \right] \exp\left[-\frac{\lambda_0}{2}(x_0 - \mu)^2 \right] \\
&\quad \propto \exp\left[\sum_{i=1}^{N} \left(-\frac{\lambda_i}{2} \{(x_i - \mu)^2 + \theta[y_i - \nu - \beta(x_i - \mu)]^2\} \right) - \frac{\lambda_0}{2}(x_0 - \mu)^2 \right] \\
&\quad \propto \exp\left[-\frac{1}{2} \left(\left[\lambda_0 + \sum_{i=1}^{N} \lambda_i (1 + \theta\beta^2) \right] \mu^2 - 2\mu \left\{ \sum_{i=1}^{N} [\lambda_i x_i - \theta\beta\lambda_i (y_i - \nu - \beta x_i)] + \lambda_0 x_0 \right\} \right) \right] \\
&\quad \propto \exp\left(-\frac{1}{2} \left[\lambda_0 + \sum_{i=1}^{N} \lambda_i (1 + \theta\beta^2) \right] \left\{ \mu - \frac{\sum_{i=1}^{N} [\lambda_i x_i - \theta\beta\lambda_i (y_i - \nu - \beta x_i)] + \lambda_0 x_0}{\lambda_0 + \sum_{i=1}^{N} \lambda_i (1 + \theta\beta^2)} \right\}^2 \right) \\
&\quad \propto N\left\{ \frac{\sum_{i=1}^{N} [\lambda_i x_i - \theta\beta\lambda_i (y_i - \nu - \beta x_i)] + \lambda_0 x_0}{\lambda_0 + \sum_{i=1}^{N} \lambda_i (1 + \theta\beta^2)}, \left[\lambda_0 + \sum_{i=1}^{N} \lambda_i (1 + \theta\beta^2) \right]^{-1} \right\}
\end{aligned}
$$

Full conditional for ν:

$$
\begin{aligned}
&p(\nu \mid \mu, \beta, \theta, \lambda_0, \lambda_1, \ldots, \lambda_N, x_0, x_1, \ldots, x_N, y_1, \ldots, y_N) \\
&\quad \propto \prod_{i=1}^{N} \exp\left(-\frac{1}{2} \theta\lambda_i \{\nu - [y_i - \beta(x_i - \mu)]\}^2 \right) \\
&\quad \propto \exp\left(-\frac{1}{2} \theta \sum_{i=1}^{N} \lambda_i \{\nu - [y_i - \beta(x_i - \mu)]\}^2 \right) \\
&\quad \propto \exp\left(-\frac{1}{2} \theta \left\{ \sum_{i=1}^{N} \lambda_i \nu^2 - 2\nu \sum_{i=1}^{N} \lambda_i [y_i - \beta(x_i - \mu)] \right\} \right) \\
&\quad \propto \exp\left(-\frac{1}{2} \left(\theta \sum_{i=1}^{N} \lambda_i \right) \left\{ \nu - \frac{\sum_{i=1}^{N} \lambda_i [y_i - \beta(x_i - \mu)]}{\sum_{i=1}^{N} \lambda_i} \right\}^2 \right) \\
&\quad \propto N\left\{ \frac{\sum_{i=1}^{N} \lambda_i [y_i - \beta(x_i - \mu)]}{\sum_{i=1}^{N} \lambda_i}, \left(\theta \sum_{i=1}^{N} \lambda_i \right)^{-1} \right\}
\end{aligned}
$$

APPENDIX B

Gibbs Sampling Algorithm

Step 1. Pick a starting value for the Markov chain: $(\mu, \nu, \beta, \theta, \lambda_0, \lambda_1, \ldots, \lambda_N)$, say

$$\left(\frac{1}{N}\sum_{i=1}^{N} x_i, \frac{1}{N}\sum_{i=1}^{N} y_i, 0, 0.9, 0.9, 0.7, \ldots, 0.7\right).$$

Step 2. Update each parameter in turn:

(i) Sample a value of θ from its full conditional distribution: $p(\theta \mid \mu, \nu, \beta, \lambda_0, \lambda_1, \ldots, \lambda_N, x_0, x_1, \ldots, x_N, y_1, \ldots, y_N)$, using the most up-to-date values of all the remaining parameters.

(ii) Sample a value of β from its full conditional distribution: $p(\beta \mid \mu, \nu, \theta, \lambda_0, \lambda_1, \ldots, \lambda_N, x_0, x_1, \ldots, x_N, y_1, \ldots, y_N)$, using the most up-to-date values of all the remaining parameters.

(iii) Sample a value of λ_0 from its full conditional distribution: $p(\lambda_0 \mid \mu, \nu, \beta, \theta, \lambda_1, \ldots, \lambda_N, x_0, x_1, \ldots, x_N, y_1, \ldots, y_N)$, using the most up-to-date values of all the remaining parameters.

(iv) Sample a value of λ_i from its full conditional distribution: $p(\lambda_i \mid \mu, \nu, \beta, \theta, \lambda_0, \lambda_1, \ldots, \lambda_{i-1}, \lambda_{i+1}, \ldots, \lambda_N, x_0, x_1, \ldots, x_N, y_1, \ldots, y_N)$, using the most up-to-date values of all the remaining parameters. Repeat for $i = 1, 2, \ldots, N$.

(v) Sample a value of μ from its full conditional distribution: $p(\mu \mid \nu, \beta, \theta, \lambda_0, \lambda_1, \ldots, \lambda_N, x_0, x_1, \ldots, x_N, y_1, \ldots, y_N)$, using the most up-to-date values of all the remaining parameters.

(vi) Sample a value of ν from its full conditional distribution: $p(\nu \mid \mu, \beta, \theta, \lambda_0, \lambda_1, \ldots, \lambda_N, x_0, x_1, \ldots, x_N, y_1, \ldots, y_N)$, using the most up-to-date values of all the remaining parameters.

Step 3. Repeat step 2 $M - 1$ times to produce a Markov chain of length M.

APPENDIX C

MCMC Simulation

We run the Gibbs sampling for a total of 260 000 iterations for all parameters at each 25-km grid specified by the PRECIS model. The first 10 000 iterations are treated as random drawings in the burn-in period during which the MCMC simulation forgets about the initial values for all parameters. After that, we save only one iteration result from every 50. Thus, we can get a total of 5000 values for each parameter, representing a sample from its posterior distribution. Estimated changes of Tmax, Tmean, and Tmin at nine probability levels (10%, 20%, . . . , 90%) for three 30-yr periods (2020–49, 2049–69, and 2070–99), calculated based on the CDFs of MCMC samples, are available online at http://env.uregina.ca/moe/pdownload.

REFERENCES

Allen, M. R., P. A. Stott, J. F. B. Mitchell, R. Schnur, and T. L. Delworth, 2000: Quantifying the uncertainty in forecasts of anthropogenic climate change. *Nature,* **407,** 617–620, doi:10.1038/35036559.

Barnett, D. N., S. J. Brown, J. M. Murphy, D. M. H. Sexton, and M. J. Webb, 2006: Quantifying uncertainty in changes in extreme event frequency in response to doubled CO_2 using a large ensemble of GCM simulations. *Climate Dyn.,* **26,** 489–511, doi:10.1007/s00382-005-0097-1.

Barnston, A. G., S. J. Mason, L. Goddard, D. G. Dewitt, and S. E. Zebiak, 2003: Multimodel ensembling in seasonal climate forecasting at IRI. *Bull. Amer. Meteor. Soc.,* **84,** 1783–1796, doi:10.1175/BAMS-84-12-1783.

Bellprat, O., S. Kotlarski, D. Lüthi, and C. Schär, 2012: Exploring perturbed physics ensembles in a regional climate model. *J. Climate,* **25,** 4582–4599, doi:10.1175/JCLI-D-11-00275.1.

Benestad, R. E., 2004: Tentative probabilistic temperature scenarios for northern Europe. *Tellus,* **56A,** 89–101, doi:10.1111/j.1600-0870.2004.00039.x.

Brooks, S., 1998: Markov chain Monte Carlo method and its application. *J. Roy. Stat. Soc.,* **47,** 69–100, doi:10.1111/1467-9884.00117.

Collins, M., B. B. B. Booth, G. R. Harris, J. M. Murphy, D. M. H. Sexton, and M. J. Webb, 2006: Towards quantifying uncertainty in transient climate change. *Climate Dyn.,* **27,** 127–147, doi:10.1007/s00382-006-0121-0.

Furrer, R., S. R. Sain, D. Nychka, and G. A. Meehl, 2007: Multivariate Bayesian analysis of atmosphere–ocean general circulation models. *Environ. Ecol. Stat.,* **14,** 249–266, doi:10.1007/s10651-007-0018-z.

Giorgi, F., and R. Francisco, 2000: Evaluating uncertainties in the prediction of regional climate change. *Geophys. Res. Lett.,* **27,** 1295–1298, doi:10.1029/1999GL011016.

——, and L. O. Mearns, 2002: Calculation of average, uncertainty range, and reliability of regional climate changes from AOGCM simulations via the ''reliability ensemble averaging'' (REA) method. *J. Climate,* **15,** 1141–1158, doi:10.1175/1520-0442(2002)015<1141:COAURA>2.0.CO;2.

——, and ——, 2003: Probability of regional climate change based on the Reliability Ensemble Averaging (REA) method. *Geophys. Res. Lett.,* **30,** 1629, doi:10.1029/2003GL017130.

Goldstein, H., and M. J. R. Healy, 1995: The graphical presentation of a collection of means. *J. Roy. Stat. Soc.,* **158,** 175–177, doi:10.2307/2983411.

Greene, A. M., L. Goddard, and U. Lall, 2006: Probabilistic multimodel regional temperature change projections. *J. Climate,* **19,** 4326–4343, doi:10.1175/JCLI3864.1.

Harris, G. R., D. M. H. Sexton, B. B. B. Booth, M. Collins, and J. M. Murphy, 2013: Probabilistic projections of transient climate change. *Climate Dyn.,* **40,** 2937–2972, doi:10.1007/s00382-012-1647-y.

Hewitt, C. D., 2004: ENSEMBLES-based predictions of climate changes and their impacts. *Eos, Trans. Amer. Geophys. Union,* **85,** 566–566, doi:10.1029/2004EO520005.

Houghton, J. T., Y. Ding, D. J. Griggs, M. Noguer, P. J. van der Linden, X. Dai, K. Maskell, and C. A. Johnson, Eds., 2001: *Climate Change 2001: The Scientific Basis.* Cambridge University Press, 881 pp.

Jones, R. G., M. Noguer, D. C. Hassell, D. Hudson, S. S. Wilson, G. J. Jenkins, and J. F. B. Mitchell, 2004: Generating high resolution climate change scenarios using PRECIS. Met Office handbook, Exeter, United Kingdom, 40 pp. [Available online at http://www.metoffice.gov.uk/media/pdf/6/5/PRECIS_Handbook.pdf.]

Karl, T. R., and K. E. Trenberth, 2003: Modern global climate change. *Science,* **302,** 1719–1723, doi:10.1126/science.1090228.

Kendon, E. J., R. G. Jones, E. Kjellström, and J. M. Murphy, 2010: Using and designing GCM–RCM ensemble regional climate projections. *J. Climate,* **23,** 6485–6503, doi:10.1175/2010JCLI3502.1.

Knutti, R., R. Furrer, C. Tebaldi, J. Cermak, and G. A. Meehl, 2010: Challenges in combining projections from multiple climate models. *J. Climate,* **23,** 2739–2758, doi:10.1175/2009JCLI3361.1.

Krishnamurti, T. N., C. M. Kishtawal, T. E. LaRow, D. R. Bachiochi, Z. Zhang, C. E. Williford, S. Gadgil, and S. Surendran, 1999: Improved weather and seasonal climate forecasts from multimodel superensemble. *Science,* **285,** 1548–1550, doi:10.1126/science.285.5433.1548.

——, ——, Z. Zhang, T. E. LaRow, D. R. Bachiochi, C. E. Williford, S. Gadgil, and S. Surendran, 2000: Multimodel ensemble forecasts for weather and seasonal climate. *J. Climate,* **13,** 4196–4216, doi:10.1175/1520-0442(2000)013<4196:MEFFWA>2.0.CO;2.

Luo, Q., R. N. Jones, M. Williams, B. Bryan, and W. Bellotti, 2005: Probabilistic distributions of regional climate change and their application in risk analysis of wheat production. *Climate Res.,* **29,** 41–52, doi:10.3354/cr029041.

Manning, L. J., J. W. Hall, H. J. Fowler, C. G. Kilsby, and C. Tebaldi, 2009: Using probabilistic climate change information from a multimodel ensemble for water resources assessment. *Water Resour. Res.,* **45,** W11411, doi:10.1029/2007WR006674.

McSweeney, C. F., and R. Jones, 2010: Selecting members of the 'QUMP' perturbed-physics ensemble for use with PRECIS. Met Office user guide, Exeter, United Kingdom, 8 pp. [Available online at http://www.metoffice.gov.uk/media/pdf/e/3/SelectingCGMsToDownscale.pdf.]

——, ——, and B. B. B. Booth, 2012: Selecting ensemble members to provide regional climate change information. *J. Climate,* **25,** 7100–7121, doi:10.1175/JCLI-D-11-00526.1.

Mearns, L. O., W. Gutowski, R. Jones, R. Leung, S. McGinnis, A. Nunes, and Y. Qian, 2009: A regional climate change assessment program for North America. *Eos, Trans. Amer. Geophys. Union,* **90,** 311, doi:10.1029/2009EO360002.

——, and Coauthors, 2012: The North American Regional Climate Change Assessment Program: Overview of phase I results. *Bull. Amer. Meteor. Soc.,* **93,** 1337–1362, doi:10.1175/BAMS-D-11-00223.1.

Meehl, G. A., C. Covey, K. E. Taylor, T. Delworth, R. J. Stouffer, M. Latif, B. McAvaney, and J. F. B. Mitchell, 2007: The WCRP CMIP3 multimodel dataset: A new era in climate change research. *Bull. Amer. Meteor. Soc.,* **88,** 1383–1394, doi:10.1175/BAMS-88-9-1383.

Murphy, J. M., D. M. H. Sexton, D. N. Barnett, G. S. Jones, M. J. Webb, M. Collins, and D. A. Stainforth, 2004: Quantification of modelling uncertainties in a large ensemble of climate change simulations. *Nature,* **430,** 768–772, doi:10.1038/nature02771.

——, B. B. B. Booth, M. Collins, G. R. Harris, D. M. H. Sexton, and M. J. Webb, 2007: A methodology for probabilistic predictions of regional climate change from perturbed physics ensembles. *Philos. Trans. Roy. Soc.,* **A365,** 1993–2028, doi:10.1098/rsta.2007.2077.

——, and Coauthors, 2009: UK climate projections science report: Climate change projections. Met Office, Exeter, United Kingdom, 193 pp. [Available online at http://ukclimateprojections.metoffice.gov.uk/22544.]

Nakicenovic, N., and R. Swart, Eds., 2000: *Special Report on Emissions Scenarios.* Cambridge University Press, 599 pp.

New, M., A. Lopez, S. Dessai, and R. Wilby, 2007: Challenges in using probabilistic climate change information for impact assessments: An example from the water sector. *Philos. Trans. Roy. Soc.,* **A365,** 2117–2131, doi:10.1098/rsta.2007.2080.

NLWIS, cited 2007: Daily 10 km gridded climate dataset: 1961–2003 version 1.0. National Land and Water Information Service, Agriculture and Agri-Food Canada. [Available online at http://www.lib.uwaterloo.ca/locations/umd/digital/documents/ClimateDatasetDaily10kmGrids.html.]

Ontario Ministry of Energy, cited 2010: Ontario's energy system meets demand of a hot summer: McGuinty government investments create a stronger, cleaner electricity system. Ontario Ministry of Energy. [Available online at http://news.ontario.ca/mei/en/2010/09/ontarios-energy-system-meets-demand-of-a-hot-summer.html.]

Ontario Ministry of the Environment, 2011a: Climate action: Adapting to change, protecting our future, 2011. Ontario Ministry of the Environment Rep. PIBS 8291, 16 pp. [Available online at http://www.climateontario.ca/doc/workshop/2011LakeSimcoe/Climate%20Action%20Adapting%20to%20Change%20Protecting%20our%20Future.pdf.]

——, 2011b: Climate ready: Ontario's adaptation strategy and action plan, 2011–2014. Ontario Ministry of the Environment Rep. PIBS 8292e, 124 pp. [Available online at http://www.ontario.ca/environment-and-energy/climate-ready-adaptation-strategy-and-action-plan-2011-2014.]

——, 2011c: Climate progress: Ontario's plan for a cleaner, more sustainable future, Annual report 2009–2010. Ontario Ministry of the Environment Rep. PIBS 8290, 56 pp. [Available online at https://ia601901.us.archive.org/17/items/stdprod085413.ome/stdprod085413.pdf.]

Räisänen, J., and T. N. Palmer, 2001: A probability and decision-model analysis of a multimodel ensemble of climate change simulations. *J. Climate,* **14,** 3212–3226, doi:10.1175/1520-0442(2001)014<3212:APADMA>2.0.CO;2.

Rayner, N. A., P. Brohan, D. E. Parker, C. K. Folland, J. J. Kennedy, M. Vanicek, T. J. Ansell, and S. F. B. Tett, 2006: Improved analyses of changes and uncertainties in sea surface temperature measured in situ since the mid-nineteenth century: The HadSST2 dataset. *J. Climate,* **19,** 446–469, doi:10.1175/JCLI3637.1.

Robertson, A. W., U. Lall, S. E. Zebiak, and L. Goddard, 2004: Improved combination of multiple atmospheric GCM ensembles for seasonal prediction. *Mon. Wea. Rev.,* **132,** 2732–2744, doi:10.1175/MWR2818.1.

Sexton, D. M. H., J. M. Murphy, M. Collins, and M. J. Webb, 2012: Multivariate probabilistic projections using imperfect climate models part I: Outline of methodology. *Climate Dyn.,* **38,** 2513–2542, doi:10.1007/s00382-011-1208-9.

Stainforth, D. A., and Coauthors, 2005: Uncertainty in predictions of the climate response to rising levels of greenhouse gases. *Nature,* **433,** 403–406, doi:10.1038/nature03301.

Stott, P. A., and J. Kettleborough, 2002: Origins and estimates of uncertainty in predictions of twenty-first century temperature rise. *Nature,* **416,** 723–726, doi:10.1038/416723a.

Taylor, K. E., R. J. Stouffer, and G. A. Meehl, 2012: An overview of CMIP5 and the experiment design. *Bull. Amer. Meteor. Soc.,* **93,** 485–498, doi:10.1175/BAMS-D-11-00094.1.

Tebaldi, C., and R. Knutti, 2007: The use of the multi-model ensemble in probabilistic climate projections. *Philos. Trans. Roy. Soc.,* **A365,** 2053–2075, doi:10.1098/rsta.2007.2076.

——, and B. Sansó, 2009: Joint projections of temperature and precipitation change from multiple climate models: A hierarchical Bayesian approach. *J. Roy. Stat. Soc.,* **172,** 83–106, doi:10.1111/j.1467-985X.2008.00545.x.

——, R. L. Smith, D. Nychka, and L. O. Mearns, 2005: Quantifying uncertainty in projections of regional climate change: A Bayesian approach to the analysis of multimodel ensembles. *J. Climate,* **18,** 1524–1540, doi:10.1175/JCLI3363.1.

Wang, X., and Coauthors, 2013: A stepwise cluster analysis approach for downscaled climate projection—A Canadian case study. *Environ. Modell. Software,* **49,** 141–151, doi:10.1016/j.envsoft.2013.08.006.

Watterson, I. G., and P. H. Whetton, 2011: Distributions of decadal means of temperature and precipitation change under global warming. *J. Geophys. Res.,* **116,** D07101, doi:10.1029/2010JD014502.

Webb, M. J., and Coauthors, 2006: On the contribution of local feedback mechanisms to the range of climate sensitivity in two GCM ensembles. *Climate Dyn.,* **27,** 17–38, doi:10.1007/s00382-006-0111-2.

Webster, M., and Coauthors, 2003: Uncertainty analysis of climate change and policy response. *Climatic Change,* **61,** 295–320, doi:10.1023/B:CLIM.0000004564.09961.9f.

Wilby, R. L., S. P. Charles, E. Zorita, B. Timbal, P. Whetton, and L. O. Mearns, 2004: Guidelines for use of climate scenarios developed from statistical downscaling methods. IPCC, 27 pp. [Available online at http://www.ipcc-data.org/guidelines/dgm_no2_v1_09_2004.pdf.]

Wilson, S., D. Hassell, D. Hein, C. Morrell, S. Tucker, R. Jones, and R. Taylor, 2011: Installing and using the Hadley Centre regional climate modelling system, PRECIS version 1.9.3. Met Office, Exeter, United Kingdom, 157 pp. [Available online at http://www.metoffice.gov.uk/media/pdf/o/5/tech_man_vn1.9.3.pdf.pdf.]

Yokohata, T., M. J. Webb, M. Collins, K. D. Williams, M. Yoshimori, J. C. Hargreaves, and J. D. Annan, 2010: Structural similarities and differences in climate responses to CO_2 increase between two perturbed physics ensembles. *J. Climate,* **23,** 1392–1410, doi:10.1175/2009JCLI2917.1.